Received: 5 July 2023 | Revised: 22 March 2024 | Accepted: 9 April 2024

DOI: 10.1111/bph.16426

RESEARCH ARTICLE

The TREK-1 potassium channel is a potential pharmacological target for vasorelaxation in pulmonary hypertension

Réka Csáki[1] | Chandran Nagaraj[1,2] | János Almássy[1] | Mohammad Ali Khozeimeh[1] | Dusan Jeremic[3] | Horst Olschewski[4] | Alice Dobolyi[1] | Konrad Hoetzenecker[5] | Andrea Olschewski[3] | Péter Enyedi[1] | Miklós Lengyel[1]

[1]Department of Physiology, Faculty of Medicine, Semmelweis University, Budapest, Hungary

[2]Ludwig Boltzmann Institute for Lung Vascular Research, Graz, Austria

[3]Experimental Anaesthesiology, Department of Anaesthesiology and Intensive Care Medicine, Medical University of Graz, Graz, Austria

[4]Department of Internal Medicine, Division of Pulmonology, Medical University of Graz, Graz, Austria

[5]Department of Thoracic Surgery, Medical University of Vienna, Vienna, Austria

Correspondence
Péter Enyedi, Department of Physiology, Faculty of Medicine, Semmelweis University, Budapest, Hungary.
Email: enyedi.peter@semmelweis.hu

Andrea Olschewski, Experimental Anaesthesiology, Department of Anaesthesiology and Intensive Care Medicine, Medical University of Graz, Graz, Austria.
Email: andrea.olschewski@medunigraz.at

Present address
Miklós Lengyel, Cell Biology Program, Memorial Sloan Kettering Cancer Center, New York, New York, USA.

Funding information
Project no. TKP2021-EGA-24 has been implemented with the support provided by the Ministry of Innovation and Technology of Hungary from the National Research,

Abstract

Background and purpose: Pulmonary arterial hypertension (PAH) is a progressive disease in which chronic membrane potential (E_m) depolarisation of the pulmonary arterial smooth muscle cells (PASMCs) causes calcium overload, a key pathological alteration. Under resting conditions, the negative E_m is mainly set by two pore domain potassium (K_{2P}) channels, of which the TASK-1 has been extensively investigated.

Experimental Approach: Ion channel currents and membrane potential of primary cultured human(h) PASMCs were measured using the voltage- and current clamp methods. Intracellular [Ca^{2+}] was monitored using fluorescent microscopy. Pulmonary BP and vascular tone measurements were also performed *ex vivo* using a rat PAH model.

Key Results: TREK-1 was the most abundantly expressed K_{2P} in hPASMCs of healthy donors and idiopathic(I) PAH patients. Background K^+-current was similar in hPASMCs for both groups and significantly enhanced by the TREK activator ML-335. In donor hPASMCs, siRNA silencing or pharmacological inhibition of TREK-1 caused depolarisation, reminiscent of the electrophysiological phenotype of idiopathic PAH. ML-335 hyperpolarised donor hPASMCs and normalised the E_m of IPAH hPASMCs. A close link was found between TREK-1 activity and intracellular Ca^{2+}-signalling using a channel activator, ML-335, and an inhibitor, spadin. In the rat, ML-335 relaxed isolated pre-constricted pulmonary arteries and significantly decreased pulmonary arterial pressure in the isolated perfused lung.

Conclusions and Implications: These data suggest that TREK-1is a key factor in E_m setting and Ca^{2+} homeostasis of hPASMC, and therefore, essential for maintenance

Abbreviations: E_m, membrane potential; IPAH, idiopathic pulmonary arterial hypertension; MCT, monocrotaline; ML-335, (*N*-[(2,4-Dichlorophenyl)methyl]-4-[(methylsulfonyl)amino]benzamide; PA, pulmonary arterial hypertension; PASMC, pulmonary arterial smooth muscle cell.

Réka Csáki and Chandran Nagaraj contributed equally to this work.

Andrea Olschewski and Péter Enyedi contributed equally to this work.

Development and Innovation Fund, financed under the TKP2021-EGA funding scheme. This work was supported by the grant ANN142950 of the Hungarian National Research, Development and Innovation Office (NKFIH) and Austrian Science Fund (FWF) [DOI:10.55776/I6299]. Chandran Nagaraj was supported by an ERS Long Term Fellowship. János Almássy was supported by the Janos Bolyai Research Scholarship of the Hungarian Academy of Sciences.

of a low resting pulmonary vascular tone. Thus TREK-1 may represent a new therapeutic target for PAH.

KEYWORDS

ML-335, pulmonary arterial hypertension (PAH), pulmonary arterial smooth muscle cells (PASMC), spadin, TREK-1

1 | INTRODUCTION

Pulmonary arterial hypertension (PAH) is a disease, characterised by a chronic progressive increase in mean pulmonary arterial pressure, resistance, chronic depolarisation and Ca^{2+} overload of pulmonary arterial smooth muscle cells (PASMCs). All approved PAH therapies, prostanoids, endothelin receptor antagonists, phosphodiesterase 5 inhibitors and soluble guanylate cyclase stimulators, have successfully addressed the vasoconstrictive mechanisms in the pulmonary arteries, proved exercise capacity and an event-free survival (Humbert et al., 2019). However, there is still much room for improvement (Humbert et al., 2023).

Depolarisation of the resting membrane potential of primary PASMCs is a hallmark of idiopathic(I) PAH (Yuan, Aldinger, et al., 1998). This depolarisation leads to Ca^{2+} overload, vasoconstriction and excessive proliferation (Platoshyn et al., 2000). However, the mechanisms underlying this depolarisation are not yet fully understood. In addition, recent studies suggest that several ionic conductances may be altered in PASMCs from animal models of PH and from PH patients. The resting membrane potential (E_m) is set by the composition of the ionic conductances of the plasma membrane. The first and, so far, the best described ionic conductance that has an impact on E_m is potassium conductance (Boucherat et al., 2015). High potassium conductance leads to hyperpolarisation and low conductance to depolarisation. In contrast, high chloride conductance shifts E_m in the depolarised direction as a consequence the difference between the equilibrium potential of Cl- and the resting E_m of PASMCs. Studies showing increased expression and activity of Ca^{2+}-activated Cl^- channels, e.g. **TMEM16A (CaCC)** in PAH, support the importance of Cl^- channels in the disease (Boucherat et al., 2015; Forrest et al., 2012; Olschewski et al., 2014; Papp et al., 2019; Sun et al., 2012).

Among the K^+ channels, the **voltage-gated K^+ channels (K_v)** and **two-pore domain K^+ channels (K_{2P})** play an important role. Altered expression or activity of K_v channels may influence cell proliferation and cell death in PASMCs (Ekhterae et al., 2001; Krick et al., 2001). In addition to their role in cell excitability, the **K_v1.5** and **K_v2.1** channels are key regulators of acute and chronic hypoxic vasoconstriction (Archer et al., 1998). However, only K_{2P} channels are active under resting conditions, suggesting that they are more important for the resting E_m than the K_v channels (Enyedi & Czirjak, 2010).

The first K_{2P} channel described in the human small pulmonary arteries was **TASK-1**, which is encoded by the *KCNK3* gene (Ma et al., 2013; Olschewski et al., 2006). The TASK-1 current is inhibited by **endothelin-1**, a major contributor to PAH and the TASK-1 channel also requires the tyrosine kinase **c-Src** to be functionally active (Nagaraj et al., 2013). Accordingly, c-Src inhibitors have been reported to cause PAH (Montani et al., 2013). Furthermore, loss-of-function mutations in TASK-1 gene (*KCNK3*) have been identified as a rare cause of hereditary pulmonary arterial hypertension (Ma et al., 2013). Subsequent studies on *KCNK3* mutant animals revealed a phenotype that resembles pulmonary hypertension in terms of morphological and haemodynamic parameters (Antigny et al., 2016; Lambert et al., 2018, 2019). These findings suggest that the channel is an important player in the pathophysiology of PAH. On the other hand, the finding that saturating concentrations of the TASK inhibitor **anandamide** did not completely inhibit K^+ conductance, implies that other K_{2P} channels may contribute to the background K^+ currents, the resting membrane potential of PASMCs and possibly, to vascular tone (Maingret et al., 2001; Olschewski et al., 2006). It has since been reported that deficiency of **TWIK-2** leads to pulmonary hypertension via a **Rho kinase**-mediated process (Pandit et al., 2014). However, the role of

What is already known?

- PASMCs in PAH are characterised by chronic depolarisation causing Ca^{2+} overload and increasing vascular tone
- The negative membrane potential (E_m) is mainly set by potassium conductances.

What does this study add?

- TREK-1 contributes significantly to the K+ conductance and hyperpolarizes the membrane potential under physiological conditions.
- TREK-1 activation leads to vasodilation and decreases pulmonary arterial pressure in rat PAH model.

What is the clinical significance?

- TREK-1 may represent a new therapeutic target for pulmonary arterial hypertension (PAH).

other K_{2P} channels in the pulmonary circulation has not yet been investigated.

Therefore, this study aimed to explore the background K_{2P} family members in primary human PASMCs obtained from the lungs of healthy donors and IPAH patients. We demonstrate, for the first time, that **TREK-1** exhibits the highest expression of all functional K_{2P} channels in the lungs of both healthy donors and IPAH patients. We show that TREK-1 is important for the low resting tone of pulmonary arteries and that its activation significantly counteracts vasoconstriction. This might represent a new therapeutic option for pulmonary hypertension.

2 | METHODS

2.1 | Human lung tissue

Lung tissues were obtained from patients who underwent lung transplantation at the Department of Surgery, Division of Thoracic Surgery, Medical University of Vienna, Vienna, Austria. As controls, we used donor lungs not used for transplantation. All procedures were approved by the institutional ethics committee, and written informed consent was obtained from all study participants. The study protocols for tissue donation were approved by the institutional ethics committees of the Medical University of Vienna (IRB approval No 976/2010) following national law and with Good Clinical Practice/International Conference on Harmonisation guidelines. Patients with IPAH were diagnosed after extensive work-up according to current guidelines (Galie et al., 2016). The patient characteristics are shown in Table S1.

2.2 | Preparation of primary cultured human pulmonary arterial smooth muscle cells (hPASMCs)

Primary cultured human PASMCs were prepared as described earlier (Olschewski et al., 2006). The word "hPASMC" refers throughout the text to primary cultured human pulmonary arterial smooth muscle cells in the text. The adventitia from small arteries with diameters of <1 mm was carefully removed under microscopic guidance. The isolated arteries were dissected and cut open to disrupt and remove endothelium by gentle scraping with forceps. Afterwards, the smooth muscle layer was cut into sections, transferred to T75 flasks with VascuLife Complete smooth muscle cell (SMC) medium containing 10% FBS (LifeLine Cell Technology, Frederick, MD) and allowed to adhere at 37°C and 5% CO_2. After adhesion, these pieces were incubated in the SMC medium supplemented with 10% FBS until cells had formed confluent monolayers. Cells were trypsinized and used for further experiments. All experiments were performed with cells between passage number 3 and 5. SMC identity was verified by their characteristic appearance under phase-contrast microscope. The purity of hPASMCs cultures was confirmed using indirect immunofluorescent antibody staining for smooth muscle actin (at least 95% of cells stained positive) and lack of staining for **von Willebrand Factor (vWF)** as described earlier (Nagy et al., 2017) (Figure S7a), which was retained in culture throughout multiple passages (as confirmed by qPCR analysis shown in Figure S7b).

Rat pulmonary vessels were prepared similarly and layered on the surface of a cell culture dish (Nagaraj et al., 2022). SMCs were allowed to migrate out of the vessel wall and attach to the bottom of the dish. The cells were cultured further in VascuLife Complete SMC medium.

2.3 | Immunofluorescence staining and immunocytochemistry

The presence of the TREK-1 channels, alpha smooth muscle actin (αSMA) and von Willebrand Factor in human lung tissue was assessed on paraffin-embedded sections as described earlier (Nagy et al., 2017). In brief, paraffin-embedded human lung sections were de-paraffinised at 60°C and incubated in pH 9 antigen retrieval solution at 95°C, followed by blocking with 10% BSA. Then samples were incubated overnight at 4°C with the following antibodies: rabbit anti-TREK-1 (Alomone labs, Israel #Apc-047, RRID:AB_2040136), goat anti-SMA (Everest Biotech, UK, #EBO6450, RRID:AB_2223024) and mouse anti-VWF (Dako, Glostrup, Denmark, #A0082, RRID:AB_2315602) in a dilution of 1:100 in 10% BSA, followed by incubation with Alexa Fluor-488, Alexa Fluor-555 and -684-labelled secondary antibodies (Life Technologies; 1:500 in 0.1% BSA) for 45 min at room temperature. Sections were washed and mounted with **DAPI**-containing medium (Vector Laboratories). The stainings were imaged on a laser scanning confocal microscope (Zeiss LMS 510 META; Zeiss, Jena, Germany) with a PlanNeofluar (40×/1.3 Oil DIC) objective.

Immunocytochemistry was performed on hPASMCs cultured on glass-bottom chamber slides. The cells were fixed by adding 4% paraformaldehyde in PBS for 20 min. After fixation, the cells were permeabilized with a solution containing 0.1% BSA and 0.5% Triton-X100 in PBS for 30 min. Antibodies and protocols for immunostaining and imaging are detailed above. The Immuno-related procedures used comply with the recommendations made by the *British Journal of Pharmacology* (Alexander et al., 2018).

2.4 | qPCR

Quantitative PCR was used for relative quantification of the K_{2P} channels. Primer pairs were from Thermofisher Inc (the amplicon sizes were between 80 and 150 bp). TaqMan® Fast Advanced Master Mix was used to perform the PCR. The Δct values for each target gene were calculated for reference gene (β2 microglobulin) using the averaged ct values: $\Delta ct = ct_{reference} - ct_{target}$.

2.5 | Plasmids, cRNA synthesis

The cloning of mouse TASK-1/**TASK-2**/**TASK-3**, **TREK-2**, **TALK-1**, **THIK-1** and **TRESK** has been described previously (Czirjak

et al., 2004; Czirjak & Enyedi, 2006). The plasmids coding mouse TREK-1 and **TRAAK** channels were kindly provided by Professor M. Lazdunski and Dr. F. Lesage. The plasmids were linearized and used for *in vitro* cRNA synthesis using the Ambion mMESSAGE mMACHINE™ T7 *in vitro* transcription kit (Ambion, Austin, TX). The structural integrity of the RNA was checked on denaturing agarose gels.

2.6 | Preparation and microinjection of Xenopus oocytes

Xenopus laevis oocytes were prepared as previously described (Czirjak & Enyedi, 2002). For the expression of the different channels, the oocytes were injected with 57 pg to 4 ng of cRNA (depending on the channel type) 1 day after defolliculation. Injection was performed with a Nanoliter Injector (World Precision Instruments, Saratosa, FL). *X. laevis* frogs were housed in 50 L tanks with continuous filtering and water circulation. Room temperature was 19°C. Frogs were anaesthetised with 0.1% tricaine solution and killed by decerebration and pithing.

2.7 | TREK-1 silencing

For silencing experiments, primary human donor and IPAH hPASMCs were seeded at a density of 50.000–100.000 cells/35-mm dish. The next day, cells were serum-starved for 3 h, then transfected either with 100 nM siRNA against TREK-1 or with non-silencing control RNA (Santa Cruz Biotechnology, Cat.#: sc-37180) using the Effectene transfection reagent kit (Qiagen) in serum-free medium. After 6 h, the reagent mixture was replaced with Complete SMC Medium. qPCR was performed for the validation of the silencing after 72 h (Figure S1). Cells were used for patch clamp studies 72 h after transfection.

2.8 | Two-electrode voltage clamp measurements

Two-electrode voltage clamp experiments were performed 2–3 days after the microinjection of cRNA into *Xenopus* oocytes, as previously described (Czirjak et al., 2004). For each channel type the oocytes contributing to the n number (n numbers are indicated in the figure legends) were derived from at least two separate frogs. The holding potential was 0 mV. Background potassium currents were measured at the end of 300 ms-long voltage steps to −100 mV applied every 4 s. Low potassium recording solution contained (in mM): NaCl 95.4, KCl 2, $CaCl_2$ 1.8, HEPES 5 (pH 7.5, adjusted by NaOH). The high potassium solution contained 80 mM K^+ (78 mM NaCl of the low potassium solution was replaced with KCl). Solutions were applied to the oocytes using a gravity-driven perfusion system. Experiments were performed at room temperature (21°C). Data were analysed by pCLAMP 10.7 software (Molecular Devices, Sunnyvale, CA, USA).

2.9 | Whole-cell patch clamp

Whole-cell patch clamp experiments were performed as previously described (Lengyel et al., 2019). The pipette solution contained (in mM): 140 KCl, 3 $MgCl_2$, 0.05 EGTA, 1 Na_2-ATP, 0.1 Na_2-GTP and 10 HEPES (pH 7.3 adjusted with NaOH). The bath solution contained (in mM):- 140 NaCl, 3.6 KCl, 0.5 $MgCl_2$, 2 $CaCl_2$, 11 glucose and 10 HEPES (pH 7.4 adjusted with NaOH). The resting membrane potential of hPASMCs was recorded in the current clamp mode with no current injection (I = 0 mode). Recordings were not corrected for the junction potential. Membrane resistance was checked at the beginning and end of recordings and cells with an unstable membrane resistance (decrease of the measured value over the course of the recording) were discarded from the analysis. The effect of ML-335 or spadin was tested on separate set of cells after 5–10 min. Preincubation with the drugs. Whole-cell currents were measured in voltage clamp mode in independent sets of experiments. The holding potential was −80 mV, whole-cell currents were measured at the end of a 300 ms long voltage step at −100 mV in every 2 s. Leak potassium current was considered as the difference between the inward current in low (3.6 mM) and high (30 mM) extracellular [K^+] medium. Changing the [K^+] and application of ML-335 (in high K^+ medium) was done by direct perfusion.

2.10 | Calcium imaging

For Ca^{2+} imaging experiments, donor hPASMCs were plated on Ibidi 8-well μ-slides (Ibidi GmbH, Germany) coated with poly-L-lysine (Sigma-Aldrich, Germany) at a density of 5.000–10.000 cells per well. Calcium imaging experiments were performed 24–48 h after plating of the cells as previously described (Lengyel, Hajdu, et al., 2021). Cells were loaded with Fura2-AM (2 μM dissolved in recording solution, Molecular Probes, USA) for 45 min. Composition of the recording solution was identical to the low potassium bath solution that was used in the patch clamp experiments. After loading, cells were incubated in recording solution containing a TREK-1 modulator (spadin, 1 μM or ML-335, 10 μM) or vehicle control (1 ‰ distilled water or 0.3 ‰ DMSO respectively) for 10–15 min. Extracellular acidification is known to evoke a calcium signal in hPASMCs leading to vasoconstriction in the pulmonary vessels (Ketabchi et al., 2009), therefore, after recording a control period, cells were challenged by decreasing the pH of the extracellular solution (to either pH 7.05 or 6.8). At the end of each experiment, ionomycin (1 μM) was applied and cells which did not respond to this stimulus with a calcium signal were excluded from the analysis. Data presented are F340/F380 fluorescence intensity ratios normalised to the F340/F380 ratios of the control period. In the experiments when the effect of acidification was tested in the absence of extracellular Ca^{2+} or in the presence of **nifedipine** (10 μM), calcium was omitted or the Ca^{2+} channel blocker was applied together with ML-335.

2.11 | Animal models of pulmonary hypertension (PH)

Animal studies are reported in compliance with the ARRIVE guidelines (Percie du Sert et al., 2020) and with the recommendations made by the British Journal of Pharmacology (Lilley et al., 2020). The monocrotaline rat model of PAH was employed as described previously (Papp et al., 2019). The Male Sprague–Dawley rats were kept in an open cage rats using eurostandard type 4 cages. Three rats were in one cage. Food (standard housing diet from Altromin (cat#.: 1324)) and water were available ad libitum. Body (weight: approx. 250 g, Charles River) received a single subcutaneous injection of monocrotaline (MCT, 60 mg·kg-1mg/kg) or vehicle (control group). Monocrotaline stock solution of 50 mg·ml^{-1} was prepared by dissolving the drug in 1 M HCl, diluted with saline and adjusting solution pH 7.3 with 1 M NaOH. After 4 weeks of monocrotaline treatment, animals in which *ex vivo* wire myography studies of the pulmonary arteries were planned were subjected to *in vivo* hemodynamic assessments to verify the presence of pulmonary hypertension. Pulmonary hypertension in the animals whose lungs underwent *ex vivo* pulmonary haemodynamic measurements was confirmed by assessment of right ventricular hypertrophy using the Fulton index.

2.11.1 | *In vivo* haemodynamics

In vivo haemodynamics was performed under constant inhalation of 2% isoflurane/oxygen, using the closed chest technique through a small incision on the submandibular area. as described in detail previously (Papp et al., 2019). The right ventricle (RV) was catheterized via the right jugular vein using a 2 F Millar catheter (SPR-513 Millar, Houston TX, USA) and right ventricular systolic pressure was measured continuously. Another catheter was inserted into the left carotid artery to monitor systemic blood pressure (SPR-320 Millar, Houston TX, USA). During the experiment the animals were placed on heated plates.

2.11.2 | Assessment of right ventricular hypertrophy (Fulton index)

At the end of the *ex vivo* measurements, the right ventricle (RV) was dissected from the left ventricle + septum (LV + S) and both of them were weighed. Right ventricular hypertrophy was assessed by calculating the Fulton index, defined as RV weight/(LV + S weight) (Papp et al., 2019).

All animal studies conformed with the EU guidelines 2010/63/EU and were approved by the Animal Care Committee of the Medical University of Graz and the federal authorities for animal research approved the study protocol (approval numbers: BMWFW--2022-0.626.084). This procedure is classified as mild according to the EU guidelines. Progression of the disease leads to faster fatigue in animals and may lead to a decrease in physical activity, similar to that seen in humans. No further or more severe symptoms occurred. The minimum numbers of animals in each group were determined using power calculations and data from previous experiments.

2.12 | *Ex vivo* wire myography

After *in vivo* haemodynamics, the animals were deeply anaesthetised and killed by exsanguination, and the intrapulmonary arteries were harvested as described in detail here. Intrapulmonary arteries isolated from rat lungs were prepared devoid of surrounding tissue under a stereo microscope (Nagaraj et al., 2016; Skofic Maurer et al., 2020). Pulmonary arteries were mounted in a myograph equipment as described before (Nagaraj et al., 2016; Nagy et al., 2017; Papp et al., 2019). The myograph chambers were connected to force transducer units for force measurements. The chamber bath solution was physiological salt solution PSS (containing in mM: 140 NaCl, 5.5 KCl, 1.5 $CaCl_2$, 1 $MgCl_2$, 10 glucose, 0.5 Na_2HPO_4, 0.5 KH_2PO_4, 10 HEPES, pH: 7.4) equilibrated with continuous aeration of 100% oxygen. After mounting of the pulmonary arteries, they were allowed to stabilise for 45 min. To further determine the vasoactive property of the intrapulmonary arteries prepared, they were challenged with a depolarising stimulus of 120 mM KCl (KPSS; isotonic replacement of NaCl by KCl) for 15 min. Tissues exhibiting less than 1 mN contractile force upon KPSS challenge were not considered for the calculations. The pretone was induced by thromboxane receptor agonist U46619 (100 nM), the evoked vasoconstrictive response was allowed to stabilise before the addition of cumulatively increasing concentrations (1–100 μM) of ML-335. Vehicle control was also included in each experiment with preconstricted arteries. The ML-335 induced response is expressed as percentage relaxation from the maximal contraction induced by U46619 before the addition of ML-335.

2.13 | *Ex vivo* measurement of pulmonary haemodynamics

Briefly, rats were killed using an overdose (i.p.) of ketamine (200 mg·kg^{-1}) and xylazine (20 mg·kg^{-1}), and treated with heparin (1,000 U·kg^{-1}) to prevent clotting. An artificial thorax was created using a water-jacketed chamber from Hugo Sachs Elektronik. Rat lungs were ventilated with positive pressure using a tidal volume of 4 ml, 90 breaths per minute and 2 cmH_2O positive end-expiratory pressure with room air. A pre-warmed, pH-adjusted buffer consisting of 118 mM NaCl, 4.7 mM KCl, 1.2 mM KH_2PO_4, 2.5 mM $CaCl_2$, 1.2 mM $MgSO_4$, 2% BSA, 0.3% HEPES and 24 mM $NaHCO_3$ was perfused via the catheterized pulmonary artery with a peristaltic pump from Ismatec. The buffer pH was continuously monitored and adjusted to maintain a pH of 7.4 with 5% CO_2 bubbling. Meanwhile, the volume control mode ventilator module/PLUGSYS device from Hugo Sachs Elektronik was used to apply negative pressure to the closed artificial thorax to carry out ventilation. Negative pressure was adjusted to produce a tidal volume of 4 ml for inspiration and end-

expiratory pressure was kept at −2 cmH2O. Ninety breaths per minute were used and a deep inspiration was added every minute at −20 cmH_2O. The mean pulmonary arterial pressure (mPAP) was continuously monitored and expressed in mmHg, and changes in mPAP were reported as delta mPAP from the baseline. ML-335 (100 μM) induced changes in the PAP upon U46619 (30 nM) pretone(p) is expressed as percentage of vasodilation and calculated as follows (pMP-pML-335)/(pMP-pB) × 100. pB is the baseline PAP, pMP is the maximal pretone PAP and pML-335 is the PAP after the exposure of ML-335 in the presence of pretone.

2.14 | Statistics

Data are shown as individual data plots with mean. Results are expressed as mean ± s.e.m. (standard error of the mean), n numbers for each group are given in the corresponding figure legend. Statistical analyses were performed using GraphPad Prism (v. 8.0.1; GraphPad Software, La Jolla, CA). Statistical tests were selected to be appropriate for the given dataset and are specified in the corresponding figure legend. Significance is given in the figure legends. All datasets met the assumptions of the statistical test used and compared groups had similar variance. *P* values < 0.05 were considered significant. Post hoc tests were conducted only if F in ANOVA achieved $P < 0.05$. The data and statistical analysis comply with the recommendations on experimental design and analysis in pharmacology (Curtis et al., 2022).

2.15 | Materials

Chemicals of analytical grade were purchased from Sigma (St. Louis, MO, USA), Fluka (Milwaukee, WI, USA) and Merck (Whitehouse Station, NJ, USA). The sortilin-derived peptide spadin was synthesised by the MTA-ELTE Research Group of Peptide Chemistry (Budapest, Hungary), dissolved in distilled water and stored as 1 mM stock solution at −20°C. ML-355 (*N*-[(2,4-Dichlorophenyl)methyl]-4-[(methylsulfonyl)amino]benzamide) was purchased from Tocris, dissolved in DMSO and stored as a 30 mM stock solution at −20°C. T2A3 (C14H12ClNO2; 2-[(4-chloro-3-methylphenyl)amino]benzoic acid) was synthesisedby, and can be obtained from D.A. Jacobson (see ref: Lengyel et al. 2020). Ionomycin (calcium salt) was purchased from Enzo Life Sciences (Farmington, NY, USA), dissolved in DMSO as a 5-mM stock solution and stored at −20°. Details of other materials and suppliers were provided in the specific sections.

2.16 | Nomenclature of targets and ligands

Key protein targets and ligands in this article are hyperlinked to corresponding entries in the IUPHAR/BPS Guide to PHARMACOLOGY http://www.guidetopharmacology.org and are permanently archived in the Concise Guide to PHARMACOLOGY 2023/24 (Alexander et al., 2023).

3 | RESULTS

3.1 | Human pulmonary arterial smooth muscle cells (hPASMCs) from idiopathic pulmonary arterial hypertension (IPAH) lungs are depolarised compared to cells from donor lungs

First, we investigated the resting membrane potential (E_m) of the primary cultured human PASMCs (hPASMCs) in our cohort. The clinical characteristics of the subjects is given in Table S1. The E_m of hPASMCs derived from multiple donors and IPAH patients was measured under control conditions. This showed that cells from IPAH patients were significantly depolarised compared to cells from healthy donors (Figure 1, donor: −49.7 ± 3.8 mV, IPAH: −24.2 ± 1.3 mV). This is consistent with previous studies and represents a hallmark of IPAH, that accounts for the Ca^{2+} overload and increased pulmonary vascular tone (Yuan, Aldinger, et al., 1998). This initial finding motivated us to investigate the expression of K_{2P} channels in our cohort.

3.2 | TREK-1 is highly expressed in hPASMCs

The expression of K_{2P} channels, such as TREK-1, TREK-2, TASK-1, TASK-5, THIK-1, TWIK-1 and TWIK-2 was examined by RT-qPCR in hPASMCs from healthy donor lungs and the most abundantly expressed K_{2P} channels were also studied in IPAH hPASMCs. Patient characteristics are given in Table S1. The expression level of the detectable channels (ΔCT) is shown in Figure 2a. TREK1

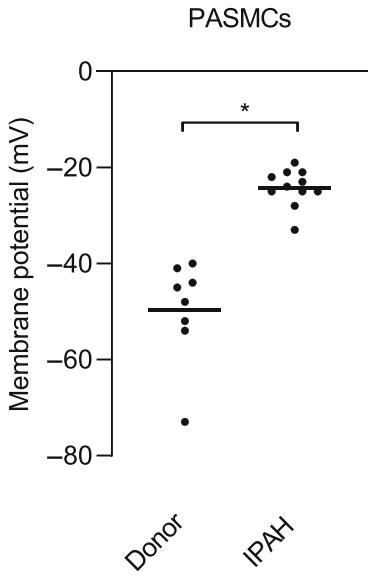

FIGURE 1 The membrane potential of idiopathic pulmonary arterial hypertension (IPAH) human pulmonary arterial smooth muscle cells (hPASMCs) are depolarised. IPAH hPASMCs were depolarised compared to cells obtained from healthy donors, n = 8 and 11 cells, respectively (*$P<0.05$, Mann–Whitney test).

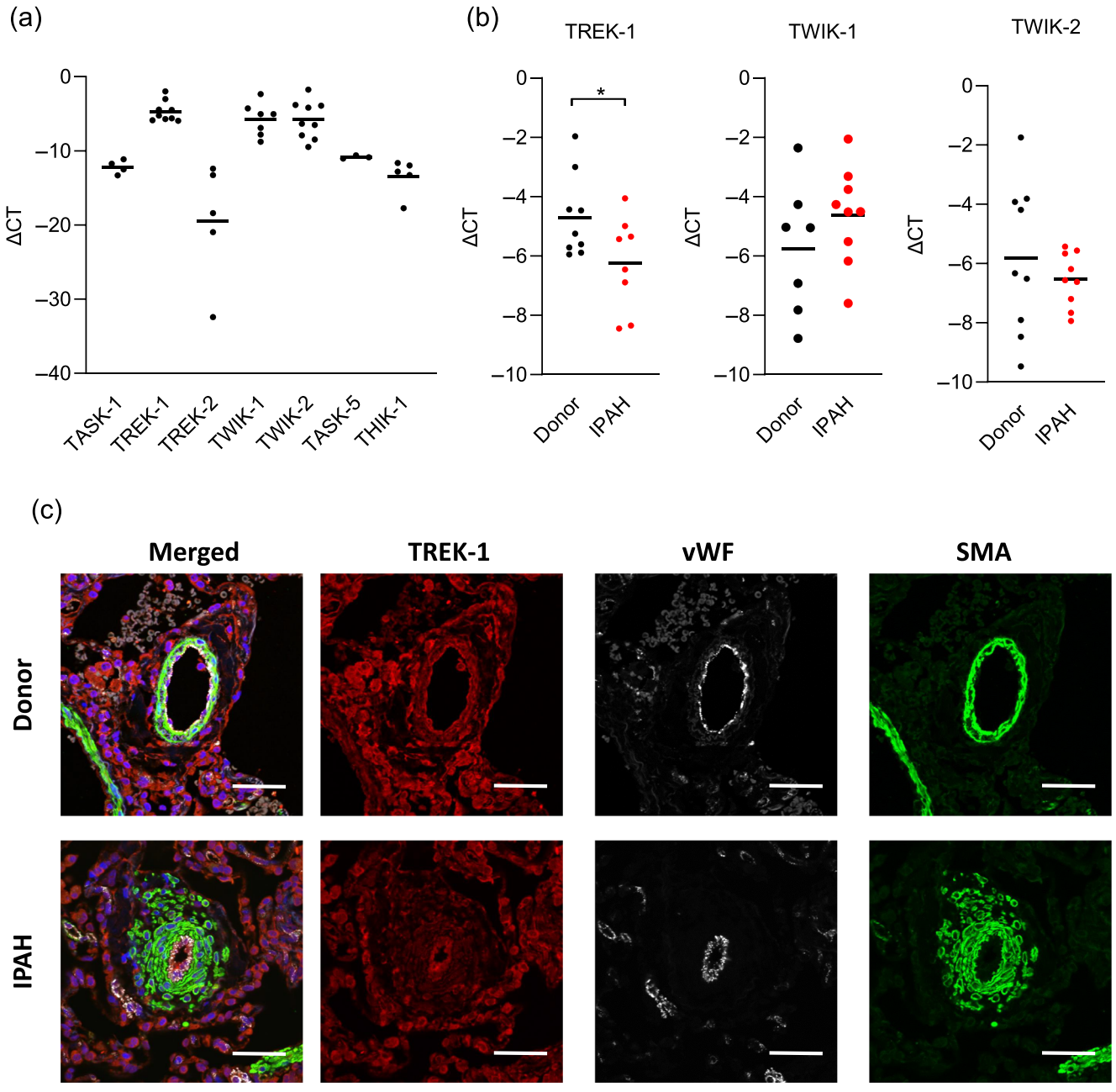

FIGURE 2 Presence of TREK-1 channels in human pulmonary arterial smooth muscle cells (hPASMCs) from donors and idiopathic pulmonary arterial hypertension (IPAH) patients. (a) Gene expression of K_{2P} family channels in hPASMCs (n = 9 donors). (b) Expression of TREK-1, TWIK-1 and TWIK-2 subunits in hPASMCs isolated from healthy donor and IPAH lungs (*$P \leq 0.05$, unpaired *t*-test, n = 8 IPAH and n = 9 healthy donors). ΔCt values were calculated by normalising the expression of target genes to β2 microglobulin expression. (c) Immunofluorescence staining for α-smooth muscle actin (α-SMA), vWF and TREK-1 in lung sections of donors and IPAH patients. Scale bar = 50 μm.

was the most highly expressed of all K_{2P} K^+ channels. In IPAH, only the expression of TREK-1 differed from that of healthy donors (with borderline statistical significance, donor ΔCT: −4.7 ± 0.5, IPAH ΔCT: −6.2 ± 0.6, Figure 2b). Localisation of the TREK-1 protein in the lungs and pulmonary vasculature was demonstrated by immunofluorescent staining of lung sections from both healthy donors and IPAH patients (Figure 2c, negative controls are shown in Figure S2).

3.3 | TREK-1 carries a substantial background K^+ current in hPASMCs

The functionality of TREK-1 channels was tested in hPASMCs from healthy donor lungs and IPAH lungs using the whole-cell patch clamp technique in voltage-clamp mode. The amplitude of the background K^+ current was assessed by measuring the inward current at −100 mV, to avoid contamination of the measurement by voltage-

dependent currents. A representative example of the time course of this experiment is shown in Figure 3a, where the data points correspond to the current amplitude measured at 2-s intervals. Since the inward K^+ currents are too small at this holding potential, they were increased by elevating the $[K^+]$ in the extracellular recording medium from 3.6 to 30 mM.

Treatment with the TREK channel activator ML-335 resulted in a significant increase in the K^+ current, which was completely reversible. The K^+ currents under control conditions and during ML-335 treatment are shown in Figure 3b. Baseline currents were not significantly different between donor and IPAH cells (donor: −2.26 ± 0.27 pA/pF, IPAH: −2.15 ± 0.39 pA/pF). Most cells responded to ML-335 treatment and ML-335 caused a significant increase in the current in both control and IPAH cells (Figure 3b, donor control: −1.95 ± 0.29 pA/pF, +ML-335: −2.97 ± 0.45 pA/pF; IPAH control: −2.27 ± 0.51 pA/pF, +ML-335: −3.25 ± 0.58 pA/pF). The extent of activation was similar in both groups (Figure 3c, donor: 1.67 ± 0.14-fold, IPAH: 1.93 ± 0.19-fold).

ML-335 was applied as a specific activator of the TREK-1 channel (Lolicato et al., 2017), but its selectivity has never been systematically

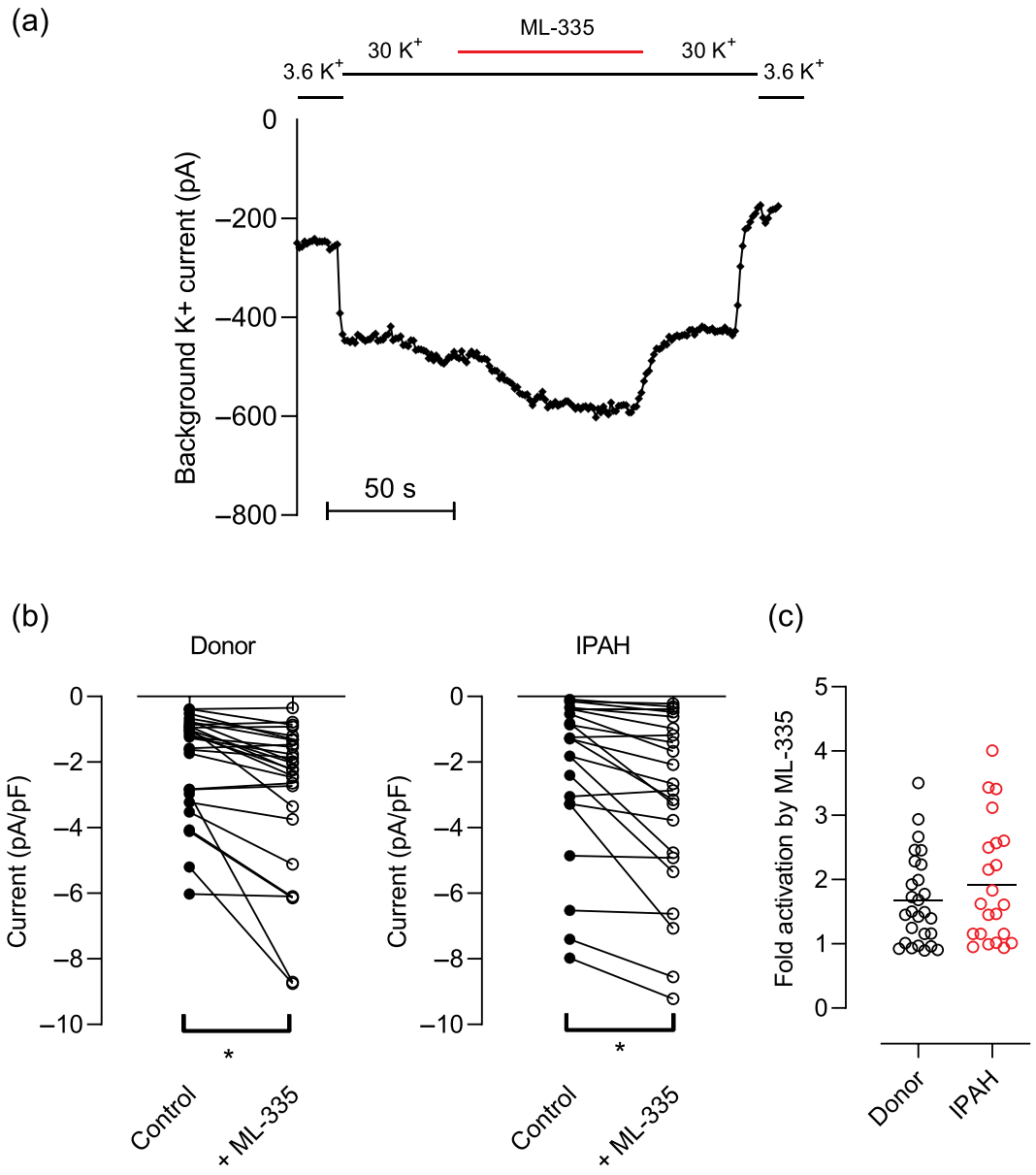

FIGURE 3 TREK-1 forms functional channels in human pulmonary arterial smooth muscle cells (hPASMCs). (a) Representative recording showing the reversible effect of ML-335 (10 μM) on the background K^+ current of a donor hPASMCs. (b) The effect of ML-335 (10 μM) on the background K^+ current of donor and idiopathic pulmonary arterial hypertension (IPAH) PASMCs (n = 27 and 22 cells, from n = 6–6 different patients, respectively). The connected data points represent measurements on the same cell, showing that ML-335 treatment significantly enhanced K^+ current in both cell types, $^*P < 0.05$, Wilcoxon signed-rank test. (c) Relative current increase upon ML-335 (10 μM) stimulation was similar in both cell types ($P > 0.05$), Mann Whitney test.

tested on other members of the K_{2P} family. To rule out the possibility that our results were due to a non-specific effect of ML-335, we examined its selectivity in a broader range of K_{2P} channels in which at least one member of each subfamily was represented. TASK-1, TASK2, TASK-3, TALK-1, TREK-1, TREK-2, TRAAK, THIK-1 and TRESK were expressed in *Xenopus* oocytes (see Figure S3 for detailed results). ML-335 (10 μM) activated only the TREK-1 and TREK-2 currents (4.8 ± 0.6-fold and 50 ± 5-fold, respectively), but not the other K_{2P} channel currents. This suggests that ML-335 is a selective ligand for TREK channels. Importantly, since TREK-2 is expressed only at very low levels in primary hPASMCs it cannot explain the ML-335-induced current. Accordingly, ML-335 can be considered as a specific TREK-1 activator in experimental models. This is supported by the fact that ML-335 ineffective in TREK-1 siRNA pretreated hPASMCs as shown in Figure 4e.

3.4 | Modulation of TREK-1 activity alters the resting membrane potential (E_m) in hPASMCs

Using the whole-cell patch-clamp technique in current-clamp mode, we tested the hypothesis that activation of TREK-1 hyperpolarises the IPAH hPASMCs. Administration of 10 μM ML-335 into the recording medium caused significant hyperpolarisation in both IPAH and donor cells, while T2A3, a specific TREK-2 activator (Dadi et al., 2017; Lengyel et al., 2020) did not (Figure 4a, donor control: −52.1 ± 2.4 mV, ML-335: −64.2 ± 2.6 mV, T2A3: −52.7 ± 1.1 mV),(Figure 4b, IPAH control: −25.5 ± 1.4 mV, ML-335: −45.3 ± 2.7 mV, T2A3: −22.3 ± 2.4 mV).

This suggests that TREK-1 but not TREK-2 controls E_m in hPASMCs. Interestingly, treatment with ML-335 hyperpolarised of IPAH cells, to the level of native donor hPASMCs.

In subsequent experiments, donor hPASMCs showed significant depolarisation after treatment with spadin (1 μM), a specific TREK-1 inhibitor (Lengyel et al., 2016; Moha ou Maati et al., 2012) (Figure 4c, control −49.6 ± 3.2 mV, spadin: −23.3 ± 2.3 mV), resulting E_m levels similar to IPAH cells.

Next, TREK-1 expression in donor hPASMCs was supressed by siRNA pretreatment, resulting in a pronounced depolarisation of E_m compared to cells treated with scrambled control siRNA (Figure 4d, siControl: −48.5 ± 2.3 mV, siTREK-1: −33.4 ± 3.2 mV). As expected, the TREK-1 activator ML-335 did not alter E_m in these cells (Figure 4e). Conversely, RNA silencing of TREK-1 did not further depolarise the IPAH hPASMCs, but eliminated the effect of ML-335, while the cells retained their sensitivity to ML-335 in the control experiments, in which they were transfected with the scrambled siRNA (Figure 4e). This suggests that ML-335 was specific for TREK-1 and that loss of TREK-1 rather than loss of another K^+ channel was the main cause of the depolarised E_m in primary IPAH hPASMCs. Activation of TREK-1 normalises the E_m of IPAH hPASMCs, but TREK-1 suppression does not lead to further depolarisation. This observation implies that the high depolarisation of E_m in IPAH cells is caused by a high Cl^- conductance, as the equilibrium potential of Cl^- is close to 0 mV under physiological ionic conditions. This is consistent with our previous findings showing that the Ca^{2+} dependent Cl^- current TMEM16A is up-regulated and functionally highly active in IPAH hPASMCs (Papp et al., 2019). All in all, we propose that, although TREK-1 is only one of the members of the unique K^+ channel repertoire of the hPASMCs plasma membrane. Further, TREK-1 is of utmost importance for membrane polarisation of hPASMCs and may represent a new pharmacological target to restore the depolarised hPASMCs membrane potential in PAH.

3.5 | TREK-1 activity modulates extracellular acidification-induced Ca^{2+} influx in hPASMCs

It has long been known that an increase in cytoplasmic [Ca^{2+}] is an important consequence of membrane depolarisation and represents an important step in the development of PAH by inducing increased muscle tone and vascular hypertrophy. We and others have previously shown that manipulation of K^+ channel activity affects Ca^{2+} signalling in hPASMCs and thus vascular tone in pulmonary arteries (Lambert et al., 2019; Nagaraj et al., 2013, 2016; Olschewski et al., 2006).

In a series of experiments, we aimed to assess the importance of TREK-1 by examining the functional connection between the membrane potential and voltage-dependent Ca^{2+} entry. We used acidosis as a gradable stimulus for hPASMCs, because it causes depolarisation and thus increased Ca^{2+} influx through voltage gated Ca^{2+} channels, leading to vasoconstriction. Although extracellular acidification directly inhibits TREK-1, this effect is moderate in the pH range we used (Cohen et al., 2008). We also verified in control experiments that TREK-1 current activation by ML-335 was similar at pH 6.8 and pH 7.4 (Figure S4).

We presumed that if TREK-1 channels have a biologically significant impact on the membrane potential, modulation of channel activity should influence the Ca^{2+} response to acidosis. To test this hypothesis donor cells were loaded with a ratiometric fluorescent Ca^{2+} indicator (Fura2-AM) and then treated with either the TREK-1 inhibitor spadin (1 μM) or vehicle (control) for 10–15 min. Afterwards, the cells were then stimulated by changing the pH of the extracellular medium from 7.40 to 7.05. This moderate acidosis increased the Fura2-AM 340/380 ratio to 1.48 ± 0.09 fold, relative to the value measured at pH 7.4 in the control (vehicle treated cells), whereas spadin pretreatment enhanced the response to 2.02 ± 0.11 fold (Figure 5b). This demonstrates that in hPASMCs, the baseline TREK-1 activity tends to protect the cells from Ca^{2+} entry. Representative traces of Ca^{2+} imaging (relative change in fluorescence ratio) are shown in Figure 5a. Next, the effect of TREK-1 activation was tested. Donor hPASMCs were pretreated with 10 μM ML-335, followed by changing the pH of the extracellular solution to 6.8. The reason why we decided to use stronger acidification in these experiments was our aim to evoke stronger depolarisation at which the hyperpolarising ML-335 has more room to reduce the Ca^{2+} signal. Indeed, acidification to pH 6.8 elicited a stronger Ca^{2+} signal in the control (vehicle treated) hPASMCs 1.91 ± 0.06 fold Fura2-AM fluorescence ratio relative to the pH 7.4 value. Consistent with the previous experiment, the

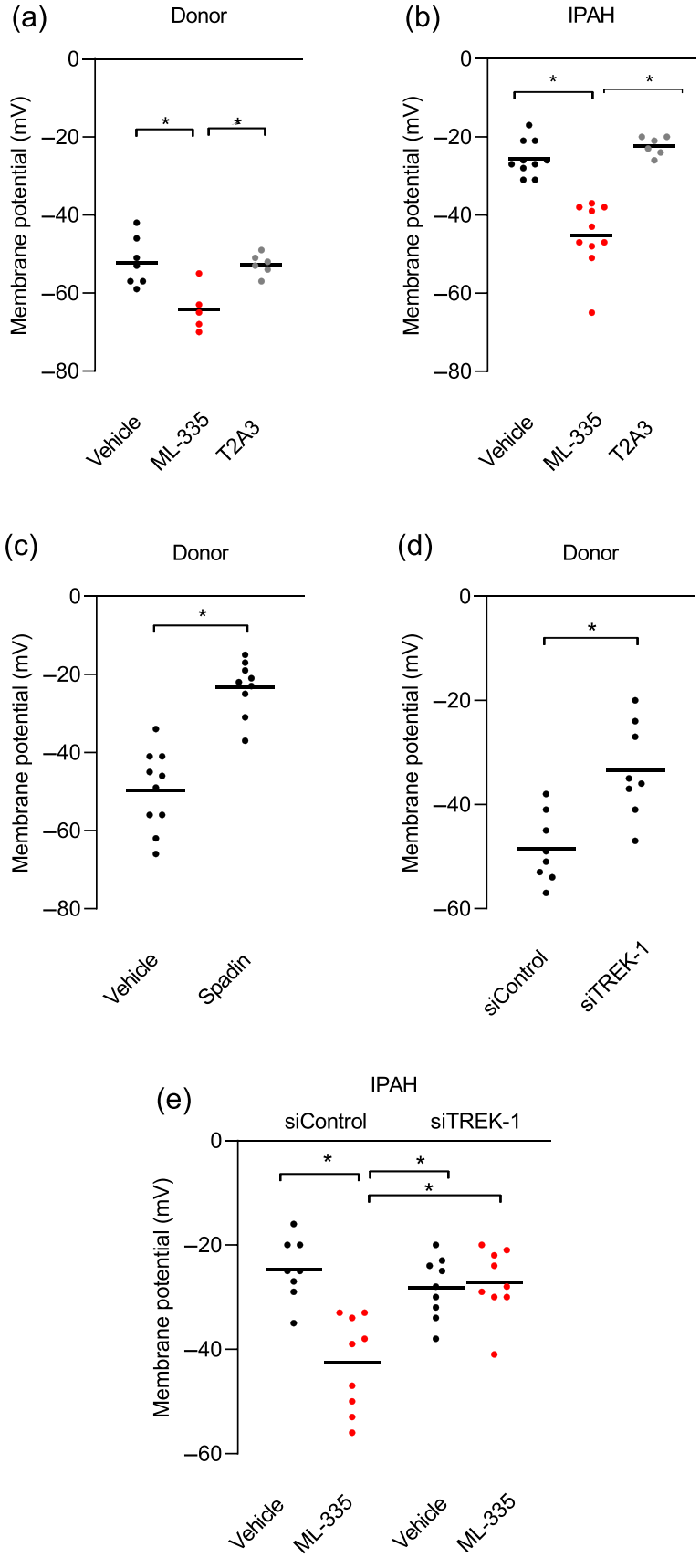

FIGURE 4 Effect of TREK-1 activity on the resting membrane potential of human pulmonary arterial smooth muscle cells (hPASMCs). The resting membrane potential was measured using the I = 0 mode of the whole-cell configuration of the patch clamp technique. (a) ML-335 (10 μM) pretreatment in hPASMCs from donors hyperpolarised the membrane potential compared to vehicle and also to the selective TREK-2 activator T2A3 (10 μM) pretreatment, n = 7, 5 and 6 cells, from n = 3 different donors, respectively, *$P < 0.05$, one-way ANOVA, followed by Tukey's post hoc test. (b) ML-335 (10 μM) pretreatment in idiopathic pulmonary arterial hypertension (IPAH) hPASMCs hyperpolarised the membrane potential compared to vehicle and also to T2A3 (10 μM) pretreatment, n = 10, 10 and 6 cells, respectively, from two different IPAH patients, *$P < 0.05$, one-way ANOVA, followed by Tukey's post hoc test. (c) Pretreatment with spadin (1 μM) in donor hPASMCs depolarised the membrane potential compared to the vehicle, n = 10 and 9 cells, respectively, from n = 3 different donors, * $P \leq 0.05$, unpaired *t*-test. (d) Silencing TREK-1 in donor hPASMCs depolarised the membrane potential, n = 8 and 8 cells, respectively, from two different donors, *$P < 0.05$, unpaired *t*-test. (e) The effect of ML-335 (10 μM) on IPAH hPASMCs after silencing TREK-1 with siRNA; n = 8–9 cells from two different IPAH patients, *$P < 0.05$, one-way ANOVA, followed by Tukey's post hoc test.

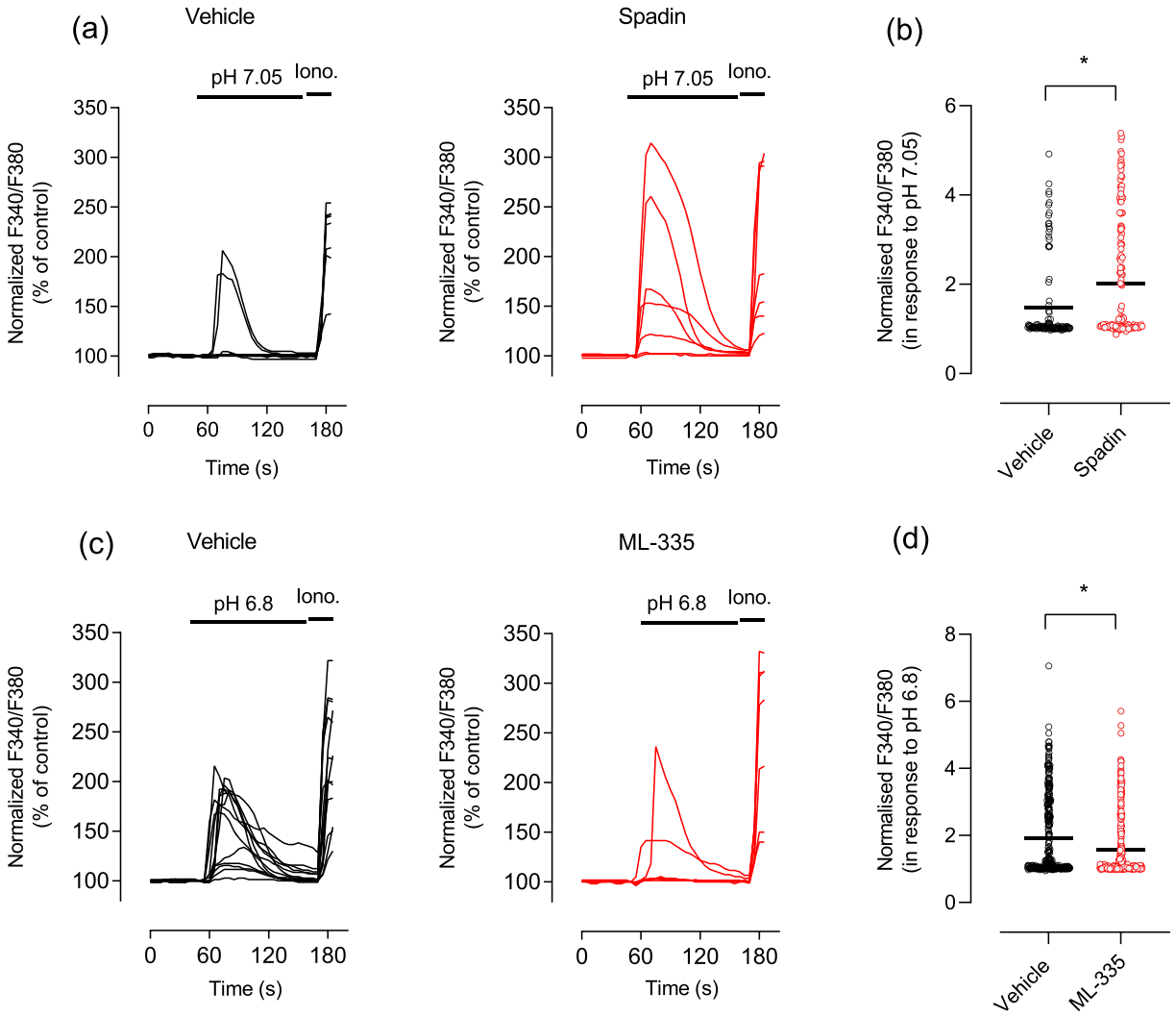

FIGURE 5 Modulation of TREK-1 activity affects calcium signal in human pulmonary arterial smooth muscle cells (hPASMCs). (a) Representative recordings of calcium imaging of hPASMCs from a single microscopic field; left panel: control cells (n = 8 cells), right panel: cells pretreated with spadin (1 μM, n = 8 cells) showing the effects of extracellular acidification (pH = 7.05) and response to the addition of 1 μM ionomycin (Iono.) The time courses of test stimuli are marked with horizontal bars above the graphs. (b) Alteration of the intracellular [Ca^{2+}] in donor hPASMCs in response to extracellular acidification after preincubation with vehicle (n = 107) or spadin (n = 138; 1 μM). *P < 0.05, Mann Whitney test, from two different donors. (c) Representative recordings of calcium imaging of hPASMCs from a single microscopic field are shown; left panel: control cells (n = 14 cells), right panel: cells pretreated with ML-335 (10 μM, n = 11 cells). Acidification (pH = 6.8) of the extracellular medium and the application of the 1 μM ionomycin test stimulus are marked with horizontal bars above the graphs. (d) Alteration of the intracellular [Ca^{2+}] of donor hPASMCs in response to extracellular acidification after preincubation with vehicle (n = 301) or ML-335 (n = 266; 10 μM). *P < 0.05, Mann Whitney test, from two different donors.

fluorescence ratio change was significantly lower in the ML-335 group than in the vehicle control group 1.56 ± 0.06 fold (Figure 5d). Representative tracings are shown in Figure 5c. The calcium signal evoked by acidosis derived exclusively from the extracellular space, partly through voltage dependent Ca^{2+} channels (Figure S5).

In summary, consistent with our resting membrane potential data, TREK-1 inhibition enhanced Ca^{2+} responses, while activation of the channel suppressed Ca^{2+} responses evoked by extracellular acidification. We conclude that the TREK-1 current in hPASMCs is strong enough to primarily cause a strongly negative resting membrane potential, which is typical of healthy donor hPASMCs. TREK-1 conductance can be pharmacologically activated to the extent that it overcomes the depolarising effects of extracellular acidification.

3.6 | TREK-1 activation causes rapid pulmonary arterial relaxation *in vitro* and a decrease in mean pulmonary arterial pressure in perfused rat lungs

The finding that our TREK-1 agonist reverses the membrane depolarisation of IPAH hPASMCs prompted us to investigate the effect of this agonist on the pulmonary circulation in an animal model. Since our

target channel may be absent in animal models, as it is the case for functional TASK-1 in mice (Manoury et al., 2011), we first examined whether PASMCs from our proposed animal model expressed functional TREK-1 current. These experiments demonstrated functional TREK-1 current in PASMCs isolated from healthy rat lungs (Figure S6), suggesting that the rat is a suitable experimental model to investigate the role of TREK-1 in the pulmonary circulation *ex vivo*. To determine the effective dose for acute vasorelaxation, we examined the TREK-1 activator-mediated pulmonary artery vasodilator response *ex vivo* using a wire myograph. Rat pulmonary arteries were preconstricted with the thromboxane A2 analogue U46619 (100 nM). This vasoconstriction was significantly reduced by the application of increasing concentrations of ML-335 (from 1 to 100 μM), as shown in Figure 6a,b. The maximum relaxation effect was 69% compared to 10% in the vehicle control with an apparent half-maximal effective concentration (EC_{50}) of 30 μM (Figure 6b). Next, we investigated the maximum relaxation effect of ML-335 in rat pulmonary arteries without endothelium. The successful removal of the endothelial layer was

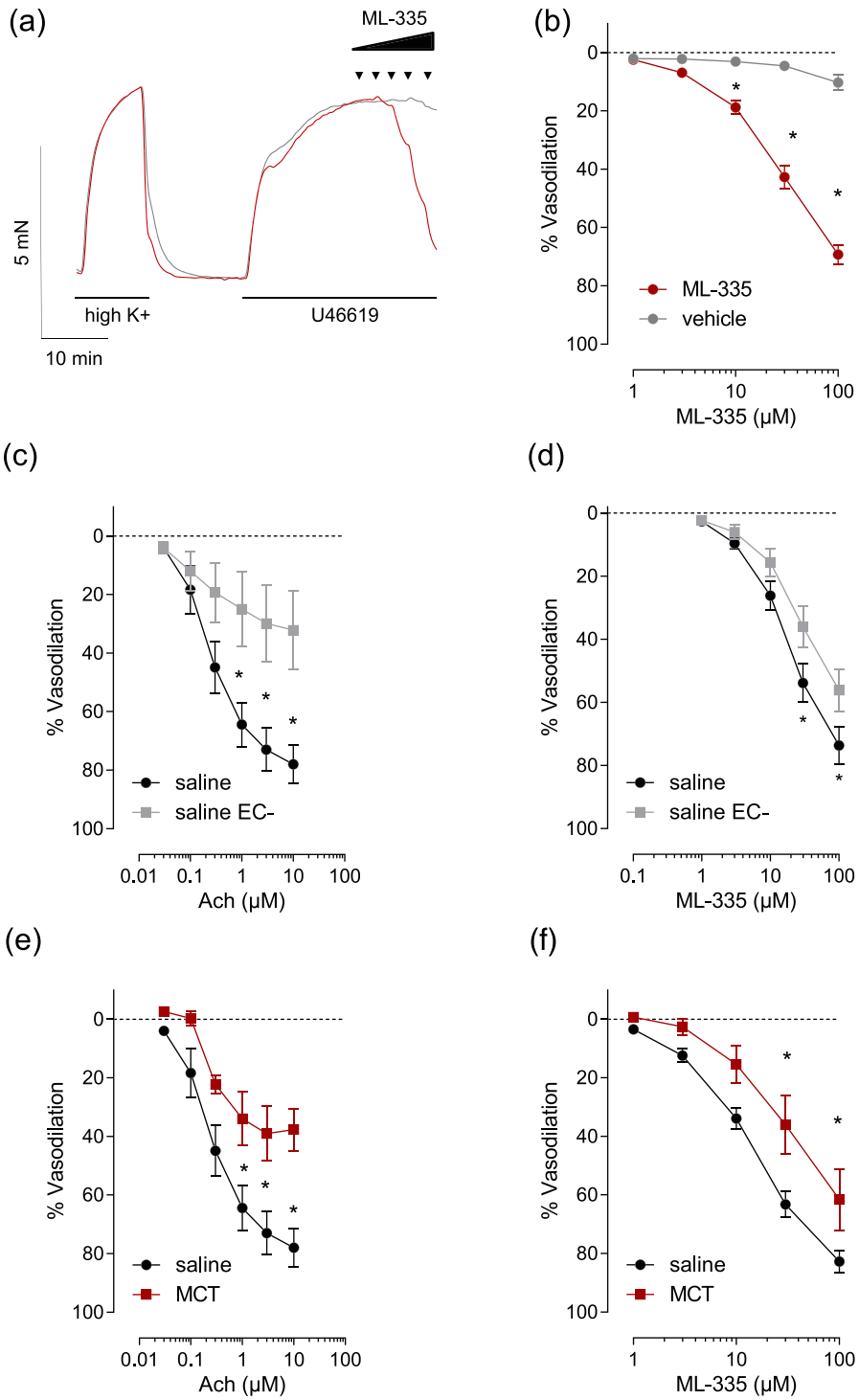

FIGURE 6 Relaxation of the pulmonary artery by activation of the TREK-1 channel. (a) Representative recordings of the tone of an isolated rat intrapulmonary artery where maximal vasoconstriction was determined by applying high [K^+] (120 mM KCl). This treatment was followed by pre-constriction with U46619 and then by cumulative concentrations of ML-335 or vehicle. (b) Dose–response curves of rat intrapulmonary arteries (n = 6). Percent vasodilation was expressed in comparison to the maximum U46619-induced vasoconstriction before ML-335 application; *P < 0.05; two-way ANOVA with Bonferroni post hoc test. (c) Dose–response curves of rat intrapulmonary arteries obtained with (black) and without endothelium (grey) (n = 8). Percent vasodilation was expressed in comparison to the maximum U46619-induced vasoconstriction before acetylcholine (Ach) application * P < 0.05; two-way ANOVA with Bonferroni post hoc test. (d) Dose–response curves of rat intrapulmonary arteries with (black) and without endothelium (grey) (n = 8). Percent vasodilation was expressed in comparison to the maximum U46619-induced vasoconstriction prior to ML-335 application *P < 0.05. Two-way ANOVA with Bonferroni post hoc test. (e) Dose–response curves of rat intrapulmonary arteries derived from saline or monocrotaline (MCT)-treated animals (n = 8). Percent vasodilation was expressed in comparison to the maximum U46619-induced vasoconstriction before acetylcholine (Ach) application *P < 0.05. Two-way ANOVA with Bonferroni post hoc test. (f) Dose–response curves of intrapulmonary arteries obtained from rats treated with saline or MCT-treated animals (n = 8). Percent vasodilation was expressed in comparison to the maximum U44619-induced vasoconstriction prior to ML-335 application. *P < 0.05 two-way ANOVA with Bonferroni post hoc test.

confirmed by the reduced acetylcholine (ACh)-mediated vasorelaxation (Figure 6c). In the absence of intact endothelium the effect of ML-335 was significantly lower (Figure 6d). Isometric tension measurements in rat pulmonary arteries derived from monocrotaline (MCT)-treated animals demonstrated attenuated ACh-mediated vasorelaxation, indicating endothelial dysfunction in this model (Figure 6e). Nevertheless, ML-335 produced dose-dependent vasodilation in these vessels too, when the isolated pulmonary arteries were preconstricted with U46619 (Figure 6f).

To gain further insight into the therapeutic relevance of TREK-1 activation, we investigated the effect of ML-335 in isolated, perfused and ventilated lungs from MCT-treated rats. Saline-treated animals served as controls. Figure 7a shows that the right ventricle/left ventricle+septum weight-ratio was significantly increased in MCT-treated rats (0.77 ± 0.08) compared to control (0.28 ± 0.01), indicating that the MCT-treatment induces right ventricular hypertrophy as a result of pulmonary hypertension. Figure 7b shows a representative trace of pressure measurement in a control rat. Pulmonary arterial pressure of 4 mmHg was increased to 10 mmHg during treatment with U46619. Addition of ML-335 to the perfusion solution resulted in a significant reduction in the pressure. Similar responses were observed in the lungs of MCT-treated animals. The individual data points are presented in Figure 7c. While the absolute value of the ML-335-dependent pressure drop was more pronounced in the MCT than in the control rats, the relative change was not statistically significantly between the two groups (saline-treated: 21.2 ± 3.1%; MCT-treated: 33.9 ± 6.3%) (Figure 7d).

4 | DISCUSSION

In our present work, the functional role of TREK-1 in sustained membrane depolarisation in IPAH was investigated and defined for the first time. First, we showed that the mechanosensitive member of the K_{2P} family TREK-1 is highly expressed and active in hPASMCs from healthy donors, and is important for the maintenance of highly negative resting membrane potential. Using a specific pharmacological activator, we demonstrated that TREK-1 contributes to the inhibition of Ca^{2+} entry in hPASMCs and to low pulmonary arterial resting tone. Second, we investigated the role of TREK-1 in IPAH and found that the TREK-1 expression is reduced in this disease while channel function remains unchanged. Moreover, significant relaxation was

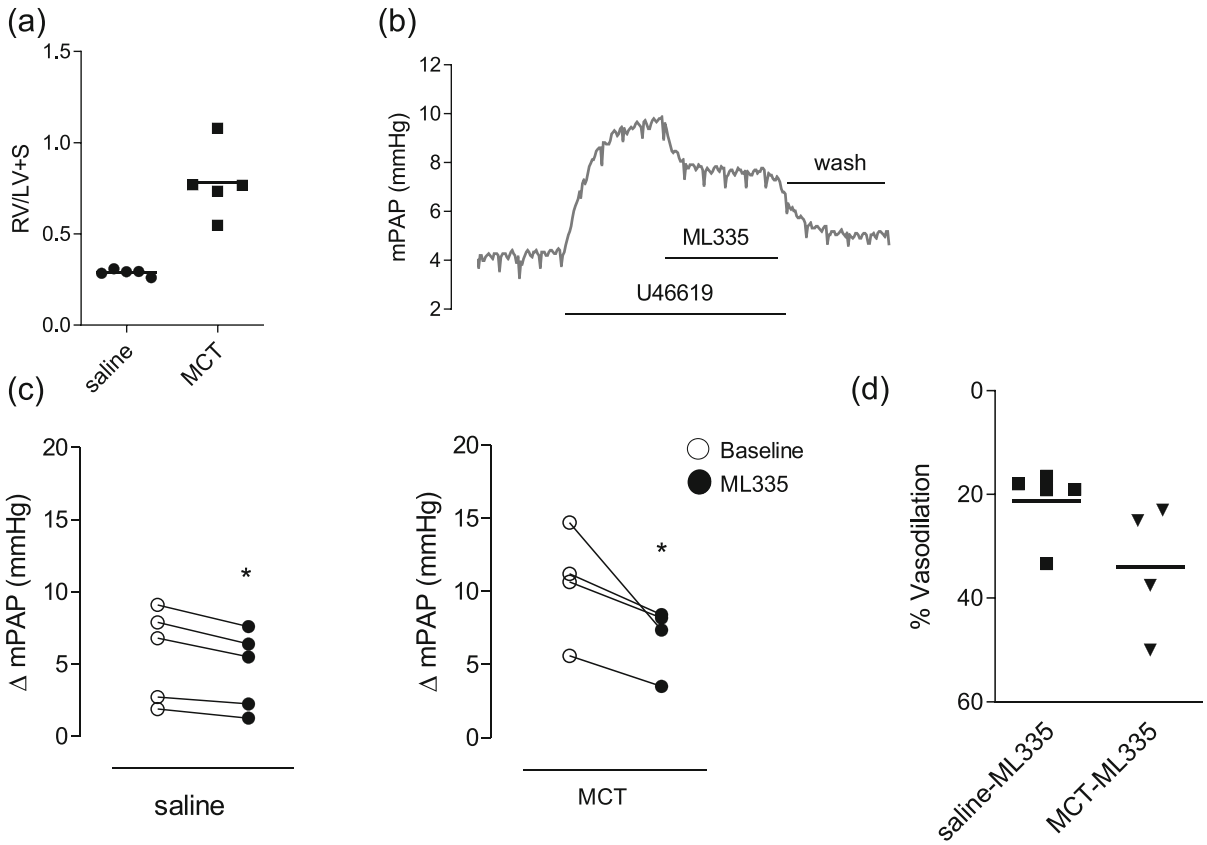

FIGURE 7 Activation of the TREK-1 channel by ML-335 induces pulmonary vasodilation in the pulmonary hypertension (PH) animal model. (a) Evaluation of right ventricular hypertrophy (Fulton index: the weight ratio of the right ventricle (RV) to the left ventricle (LV) plus septum (S)) of saline (n = 5) and monocrotaline (MCT; n = 5) treated rats. (b) Representative traces of mPAP of an *ex-vivo* lung perfused with ML-335 in the presence of U46619. (c) Summarised mPAP before (open circle) and after ML-335 administration (closed circle) in control (saline-treated, n = 5) and MCT treated rats (n = 4). Each data point represents one animal. *P < 0.05, paired t test. (d) Summarised ML-335-induced relative vasodilation in control animals (saline-treated, n = 5) and MCT treated animals (n = 4). Each data point represents one animal.

observed in a PAH animal model by increasing TREK-1 activity, strongly suggesting that enhancing TREK-1 activity is a novel option to reduce pulmonary vascular tone. Our data provide new mechanistic insights into how change in TREK-1 activity alters the vascular tone and introduces TREK-1 as a valuable therapeutic target.

The aim of our study was to gain further insight into the role of K_{2P} channels in hPASMCs and in pulmonary arterial hypertension. PAH is characterised by functional dysregulation and structural remodelling of the small precapillary arteries. Haemodynamically, PAH is defined as a mean pulmonary arterial pressure of >20 mmHg, pulmonary arterial wedge pressure ≤15 mmHg and PVR ≥ 2.0 Wood units (Humbert et al., 2019, 2023). A hallmark of the pathology is chronic membrane depolarisation of PASMCs leading to activation of Ca^{2+} channels, e.g. voltage-gated Ca^{2+} channels and consequently causes excess influx of Ca^{2+}. In severe PAH, the increased vascular tone results in elevated pulmonary vascular resistance and pulmonary arterial pressure. The activity of the K^+ channels of the PASMCs plasma membrane strongly contributes to the negative membrane potential and thus to the low pulmonary vascular tone. Yuan et al. have shown that the expression of the alpha-subunit of the voltage-gated $K_v1.5$ channel was decreased in IPAH (formerly primary PH), but the functional role of this channel in the resting membrane potential and vascular tone has not been demonstrated (Yuan, Aldinger, et al., 1998; Yuan, Wang, et al., 1998). It is noteworthy that Kv1.5 is strongly voltage dependent and is not active at the physiological membrane potential of PASMCs. More importantly, a recent study showed enhanced expression of the regulatory KCNE subunit of the **Kv7 channel** in PAH-PASMCs and PASMCs from an animal model of PH, highlighting the potential role of Kv7 in the patho-mechanism of PH (Mondéjar-Parreño et al., 2020). Interestingly, pulmonary arteries obtained from healthy animals showed virtually no response to Kv7 channel modulators in this study, whereas the same inhibitor induced strong vasoconstriction in the same animal model in a previous study (Joshi et al., 2009). Therefore, further studies on Kv7 channels in the pulmonary arteries are warranted. Background K_{2P} channels are expressed in the systemic circulation and play a physiological role in controlling resting membrane potential and tone in rodents (Blondeau et al., 2007; Bryan et al., 2006; Garry et al., 2007). In contrast, our knowledge about their role in the human pulmonary circulation is still limited. We have previously shown that the K_{2P} channel TASK-1, encoded by *KCNK3*, is active at resting membrane potential and that it is inhibited by endothelin-1 and hypoxia in PASMCs, accounting at least partially for the membrane depolarisation in IPAH (Nagaraj et al., 2013; Olschewski et al., 2006; Tang et al., 2009). TASK-1 has attracted further attention in the human pulmonary circulation as missense mutations can lead to hereditary PAH (Ma et al., 2013). Other comparative studies revealed significant species variation in the expression pattern of the TASK-1 channel in the pulmonary vessels and reported that the channel, which has been shown to be important in humans, is dysfunctional or even absent in mouse PASMCs (Manoury et al., 2011; Murtaza et al., 2017). Finally, studies employing genetically modified rats have shown that *KCNK3*-inactivation leads to remodelling of the pulmonary vasculature and favours the development of PH in an age-dependent manner (Lambert et al., 2019). Therefore, it is important to further determine the expression and function of K_{2P} in PASMCs to better define the overall role of these unique channels in pulmonary vascular homeostasis under normal and PAH conditions.

In line with previous studies, our investigations show significant depolarisation of hPASMCs derived from IPAH patients. The membrane potential of hPASMCs *in vitro* is about −50 mV (Papp et al., 2019; Platoshyn et al., 2004). At this membrane potential, all K_{2P} channels are active and should contribute to setting the resting membrane potential. Therefore, we first screened the K_{2P} channel expression in hPASMCs and found that TREK-1 was the most highly expressed channel. TREK-1 is a particularly interesting member of the K_{2P} family and may be of great importance for the pulmonary circulation as it is activated by mechanical stretch, **arachidonic acid** and other polyunsaturated fatty acids, and is the target of receptor mediated regulation (Lengyel, Enyedi, & Czirjak, 2021; Patel et al., 1998). The mechanosensitivity of TREK-1 lies within the physiological range of pressures in the pulmonary circulation (Brohawn et al., 2014; Glogowska et al., 2021), suggesting that TREK-1 activation and subsequent hyperpolarisation may play a role in the physiological pressure-induced vasodilation of pulmonary arteries. Furthermore, TREK-1 is moderately sensitive to extracellular acidification and, like several other K_{2P} channels, can be activated by volatile anaesthetics (Miller et al., 2003). Interestingly, the expression of TREK-1 mRNA was down-regulated in IPAH, whereas this was not the case for the other K_{2P} channels. By manipulating TREK-1 channel activity with pharmacological agents or reducing the expression with siRNA, we were able to show that the channel strongly contributes to the resting membrane potential of hPASMCs. Reducing channel expression with siRNA led to substantial depolarisation of the resting membrane potential of donor hPASMCs. The same was observed when TREK-1 was inhibited by the specific channel inhibitor spadin. Both treatments simulated a condition similar to the IPAH phenotype in hPASMCs. On the other hand, ML-335, a TREK-1 and TREK-2 activator, hyperpolarised both donor and IPAH hPASMCs, while a selective TREK-2 activator showed no effect. These effects, as well as the high expression of TREK1 and low expression of TREK2 mRNA, suggest that the resting membrane potential of hPASMCs depends on TREK-1 but not on TREK-2. In IPAH hPASMCs, hyperpolarisation by ML-335 led to membrane potential values comparable to those of donor hPASMCs. This effect did not manifest in TREK-1-silenced IPAH cells, again confirming that the effect of ML-335 in hPASMCs is mediated by TREK-1.

Increased cytoplasmic Ca^{2+} concentration is an important downstream consequence of membrane depolarisation and a crucial step in the development of PH. We and others have previously shown that manipulating the activity of K^+ channels alters Ca^{2+} signalling in hPASMCs and, accordingly, vascular tone in pulmonary arteries (Lambert et al., 2019; Nagaraj et al., 2013, 2016; Olschewski et al., 2006). In this study, we examined the effects of TREK-1 modulation on Ca^{2+} signalling induced by extracellular acidification. We applied either mild (pH 7.05) or moderate (pH 6.8) acidosis to induce a Ca^{2+}signal, in order to show that both inhibition and activation of

TREK-1 influences the Ca^{2+} homeostasis of the cells, respectively. We have shown that TREK-1 is only slightly regulated in this pH range and thus, it still can be robustly activated under acidic conditions. Consistent with the observations on the resting membrane potential, inhibition of TREK-1 promoted Ca^{2+} responses, whereas activation of the channel attenuated the response to extracellular acidification.

Alterations in the expression and function of various K^+ channels, and thus an abnormal Ca^{2+} balance, have previously been linked to the pathogenesis of pulmonary arterial remodelling (Humbert et al., 2019). Here, we updated these theories and demonstrated that TREK-1 is also involved in the regulation of pulmonary vascular tone. To gain further insight into the potential therapeutic relevance of TREK-1 activation, we examined the effects of acute administration of ML-335 on preconstricted intrapulmonary arteries, a model that involves increased pulmonary vascular resistance thus mimicking crucial aspects of the human disease. Consistent with the effects observed on the membrane potential- and intracellular Ca^{2+} concentrations, TREK-1 activation resulted in a strong dose-dependent relaxation of the intrapulmonary arteries. The observed vasodilation depended on both smooth muscle and endothelial cells. Furthermore, ML-335 induced a strong vasorelaxation in isolated pulmonary arteries, which was confirmed by experiments using isolated, perfused and ventilated lungs of animals treated with monocrotaline (MCT). These results suggest that TREK-1 has a high therapeutic potential in diseases with pulmonary vasoconstriction.

5 | CONCLUSIONS

The present study is the first to functionally characterise TREK-1 in the pulmonary circulation. We demonstrate the important role of TREK-1 for setting the negative membrane potential in primary human and rat PASMC with functional consequences on Ca^{2+} signalling. Also, we demonstrate the relaxing effect of TREK-1 conductance on pulmonary arteries of rats with pulmonary hypertension and that pharmacological activation of TREK-1 lowers the pulmonary arterial pressure. Our results suggest that TREK-1 is important for low resting pulmonary tone and that its activation has therapeutic potential. TREK-1 appears to be a new pharmacological target for pulmonary hypertension.

AUTHOR CONTRIBUTIONS

Reka Csaki: Formal analysis (equal); investigation (equal); visualization (equal); writing—review and editing (equal). **Chandran Nagaraj:** Formal analysis (equal); investigation (equal); methodology (equal); visualization (equal); writing—original draft (equal); writing—review and editing (equal). **Janos Almassy:** Investigation (supporting); writing—original draft (equal); writing—review and editing (equal). **Mohammad Ali Khozeimeh:** Investigation (supporting). **Horst Olschewski:** Writing—review and editing (equal). **Alice Dobolyi:** Investigation (supporting); project administration (equal). **Konrad Hoetzenecker:** Investigation (supporting); methodology (equal). **Andrea Olschewski:** Conceptualization (equal); funding acquisition (equal); resources (equal); supervision (equal); writing—original draft (equal); writing—review and editing (equal). **Péter Enyedi:** Conceptualization (equal); funding acquisition (equal); resources (equal); supervision (equal); writing—original draft (equal); writing—review and editing (equal). **Miklós Lengyel:** Conceptualization (equal); formal analysis (equal); investigation (equal); visualization (equal); writing—original draft (equal); writing—review and editing (equal).

ACKNOWLEDGEMENTS

The skilful technical assistance provided by Elisabeth Blanz is much appreciated.

CONFLICT OF INTEREST STATEMENT

There are no competing interests.

DATA AVAILABILITY STATEMENT

Data available on request from the authors. All study data are included in the article and supporting information.

DECLARATION OF TRANSPARENCY AND SCIENTIFIC RIGOUR

This Declaration acknowledges that this paper adheres to the principles for transparent reporting and scientific rigour of preclinical research as stated in the *BJP* guidelines for Design and Analysis, Immunoblotting and Immunochemistry and Animal Experimentation, and as recommended by funding agencies, publishers and other organisations engaged with supporting research.

ORCID

Miklós Lengyel https://orcid.org/0000-0001-6382-6369

REFERENCES

Alexander, S. P. H., Mathie, A. A., Peters, J. A., Veale, E. L., Striessnig, J., Kelly, E., Armstrong, J. F., Faccenda, E., Harding, S. D., Davies, J. A., Aldrich, R. W., Attali, B., Baggetta, A. M., Becirovic, E., Biel, M., Bill, R. M., Caceres, A. I., Catterall, W. A., Conner, A. C., … Zhu, M. (2023). The concise guide to PHARMACOLOGY 2023/24: Ion channels. *British Journal of Pharmacology*, *180*, S145–S222. https://doi.org/10.1111/bph.16178

Alexander, S. P. H., Roberts, R. E., Broughton, B. R. S., Sobey, C. G., George, C. H., Stanford, S. C., Cirino, G., Docherty, J. R., Giembycz, M. A., Hoyer, D., Insel, P. A., Izzo, A. A., Ji, Y., MacEwan, D. J., Mangum, J., Wonnacott, S., & Ahluwalia, A. (2018). Goals and practicalities of immunoblotting and immunohistochemistry: A guide for submission to the *British Journal of Pharmacology*. *British Journal of Pharmacology*, *175*, 407–411. https://doi.org/10.1111/bph.14112

Antigny, F., Hautefort, A., Meloche, J., Belacel-Ouari, M., Manoury, B., Rucker-Martin, C., Péchoux, C., Potus, F., Nadeau, V., Tremblay, E., Ruffenach, G., Bourgeois, A., Dorfmüller, P., Breuils-Bonnet, S., Fadel, E., Ranchoux, B., Jourdon, P., Girerd, B., Montani, D., … Perros, F. (2016). Potassium Channel subfamily K member 3 (KCNK3) contributes to the development of pulmonary arterial hypertension. *Circulation*, *133*, 1371–1385. https://doi.org/10.1161/CIRCULATIONAHA.115.020951

Archer, S. L., Souil, E., Dinh-Xuan, A. T., Schremmer, B., Mercier, J. C., el Yaagoubi, A., Nguyen-Huu, L., Reeve, H. L., & Hampl, V. (1998). Molecular identification of the role of voltage-gated K+ channels, Kv1.5 and Kv2.1, in hypoxic pulmonary vasoconstriction and control of resting

membrane potential in rat pulmonary artery myocytes. *The Journal of Clinical Investigation*, *101*, 2319–2330. https://doi.org/10.1172/JCI333

Blondeau, N., Pétrault, O., Manta, S., Giordanengo, V., Gounon, P., Bordet, R., Lazdunski, M., & Heurteaux, C. (2007). Polyunsaturated fatty acids are cerebral vasodilators via the TREK-1 potassium channel. *Circulation Research*, *101*, 176–184. https://doi.org/10.1161/CIRCRESAHA.107.154443

Boucherat, O., Chabot, S., Antigny, F., Perros, F., Provencher, S., & Bonnet, S. (2015). Potassium channels in pulmonary arterial hypertension. *The European Respiratory Journal*, *46*, 1167–1177. https://doi.org/10.1183/13993003.00798-2015

Brohawn, S. G., Su, Z., & MacKinnon, R. (2014). Mechanosensitivity is mediated directly by the lipid membrane in TRAAK and TREK1 K+ channels. *Proceedings of the National Academy of Sciences of the United States of America*, *111*, 3614–3619. https://doi.org/10.1073/pnas.1320768111

Bryan, R. M. Jr., You, J., Phillips, S. C., Andresen, J. J., Lloyd, E. E., Rogers, P. A., Dryer, S. E., & Marrelli, S. P. (2006). Evidence for two-pore domain potassium channels in rat cerebral arteries. *American Journal of Physiology. Heart and Circulatory Physiology*, *291*, H770–H780. https://doi.org/10.1152/ajpheart.01377.2005

Cohen, A., Ben-Abu, Y., Hen, S., & Zilberberg, N. (2008). A novel mechanism for human K2P2.1 channel gating. Facilitation of C-type gating by protonation of extracellular histidine residues. *The Journal of Biological Chemistry*, *283*, 19448–19455. https://doi.org/10.1074/jbc.M801273200

Curtis, M. J., Alexander, S. P. H., Cirino, G., George, C. H., Kendall, D. A., Insel, P. A., Izzo, A. A., Ji, Y., Panettieri, R. A., Patel, H. H., Sobey, C. G., Stanford, S. C., Stanley, P., Stefanska, B., Stephens, G. J., Teixeira, M. M., Vergnolle, N., & Ahluwalia, A. (2022). Planning experiments: Updated guidance on experimental design and analysis and their reporting III. *British Journal of Pharmacology*, *179*, 3907–3913. https://doi.org/10.1111/bph.15868

Czirjak, G., & Enyedi, P. (2002). Formation of functional heterodimers between the TASK-1 and TASK-3 two-pore domain potassium channel subunits. *The Journal of Biological Chemistry*, *277*, 5426–5432. https://doi.org/10.1074/jbc.M107138200

Czirjak, G., & Enyedi, P. (2006). Zinc and mercuric ions distinguish TRESK from the other two-pore-domain K+ channels. *Molecular Pharmacology*, *69*, 1024–1032. https://doi.org/10.1124/mol.105.018556

Czirjak, G., Toth, Z. E., & Enyedi, P. (2004). The two-pore domain K+ channel, TRESK, is activated by the cytoplasmic calcium signal through calcineurin. *The Journal of Biological Chemistry*, *279*, 18550–18558. https://doi.org/10.1074/jbc.M312229200

Dadi, P. K., Vierra, N. C., Days, E., Dickerson, M. T., Vinson, P. N., Weaver, C. D., & Jacobson, D. A. (2017). Selective small molecule activators of TREK-2 channels stimulate dorsal root ganglion c-fiber nociceptor two-pore-domain Potassium Channel currents and limit calcium influx. *ACS Chemical Neuroscience*, *8*, 558–568. https://doi.org/10.1021/acschemneuro.6b00301

Ekhterae, D., Platoshyn, O., Krick, S., Yu, Y., McDaniel, S. S., & Yuan, J. X. (2001). Bcl-2 decreases voltage-gated K+ channel activity and enhances survival in vascular smooth muscle cells. *American Journal of Physiology. Cell Physiology*, *281*, C157–C165. https://doi.org/10.1152/ajpcell.2001.281.1.C157

Enyedi, P., & Czirjak, G. (2010). Molecular background of leak K+ currents: Two-pore domain potassium channels. *Physiological Reviews*, *90*, 559–605. https://doi.org/10.1152/physrev.00029.2009

Forrest, A. S., Joyce, T. C., Huebner, M. L., Ayon, R. J., Wiwchar, M., Joyce, J., Freitas, N., Davis, A. J., Ye, L., Duan, D. D., Singer, C. A., Valencik, M. L., Greenwood, I. A., & Leblanc, N. (2012). Increased TMEM16A-encoded calcium-activated chloride channel activity is associated with pulmonary hypertension. *American Journal of Physiology. Cell Physiology*, *303*, C1229–C1243. https://doi.org/10.1152/ajpcell.00044.2012

Galiè, N., Humbert, M., Vachiery, J. L., Gibbs, S., Lang, I., Torbicki, A., Simonneau, G., Peacock, A., Vonk Noordegraaf, A., Beghetti, M., Ghofrani, A., Gomez Sanchez, M. A., Hansmann, G., Klepetko, W., Lancellotti, P., Matucci, M., McDonagh, T., Pierard, L. A., Trindade, P. T., … ESC Scientific Document Group. (2016). 2015 ESC/-ERS guidelines for the diagnosis and treatment of pulmonary hypertension: The joint Task force for the diagnosis and treatment of pulmonary hypertension of the European Society of Cardiology (ESC) and the European Respiratory Society (ERS): Endorsed by: Association for European Paediatric and Congenital Cardiology (AEPC), International Society for Heart and Lung Transplantation (ISHLT). *European Heart Journal*, *37*, 67–119. https://doi.org/10.1093/eurheartj/ehv317

Garry, A., Fromy, B., Blondeau, N., Henrion, D., Brau, F., Gounon, P., Guy, N., Heurteaux, C., Lazdunski, M., & Saumet, J. L. (2007). Altered acetylcholine, bradykinin and cutaneous pressure-induced vasodilation in mice lacking the TREK1 potassium channel: The endothelial link. *EMBO Reports*, *8*, 354–359. https://doi.org/10.1038/sj.embor.7400916

Glogowska, E., Arhatte, M., Chatelain, F. C., Lesage, F., Xu, A., Grashoff, C., Discher, D. E., Patel, A., & Honoré, E. (2021). Piezo1 and Piezo2 foster mechanical gating of K2P channels. *Cell Reports*, *37*, 110070. https://doi.org/10.1016/j.celrep.2021.110070

Humbert, M., Guignabert, C., Bonnet, S., Dorfmüller, P., Klinger, J. R., Nicolls, M. R., Olschewski, A. J., Pullamsetti, S. S., Schermuly, R. T., Stenmark, K. R., & Rabinovitch, M. (2019). Pathology and pathobiology of pulmonary hypertension: State of the art and research perspectives. *The European Respiratory Journal*, *53*, 1801887. https://doi.org/10.1183/13993003.01887-2018

Humbert, M., Kovacs, G., Hoeper, M. M., Badagliacca, R., Berger, R. M. F., Brida, M., Carlsen, J., Coats, A. J. S., Escribano-Subias, P., Ferrari, P., Ferreira, D. S., Ghofrani, H. A., Giannakoulas, G., Kiely, D. G., Mayer, E., Meszaros, G., Nagavci, B., Olsson, K. M., Pepke-Zaba, J., … the ESC/ERS Scientific Document Group. (2023). 2022 ESC/ERS guidelines for the diagnosis and treatment of pulmonary hypertension. *The European Respiratory Journal*, *61*, 2200879. https://doi.org/10.1183/13993003.00879-2022

Joshi, S., Sedivy, V., Hodyc, D., Herget, J., & Gurney, A. M. (2009). KCNQ modulators reveal a key role for KCNQ potassium channels in regulating the tone of rat pulmonary artery smooth muscle. *The Journal of Pharmacology and Experimental Therapeutics*, *329*, 368–376. https://doi.org/10.1124/jpet.108.147785

Ketabchi, F., Egemnazarov, B., Schermuly, R. T., Ghofrani, H. A., Seeger, W., Grimminger, F., Shid-Moosavi, M., Dehghani, G. A., Weissmann, N., & Sommer, N. (2009). Effects of hypercapnia with and without acidosis on hypoxic pulmonary vasoconstriction. *American Journal of Physiology. Lung Cellular and Molecular Physiology*, *297*, L977–L983. https://doi.org/10.1152/ajplung.00074.2009

Krick, S., Platoshyn, O., Sweeney, M., Kim, H., & Yuan, J. X. (2001). Activation of K+ channels induces apoptosis in vascular smooth muscle cells. *American Journal of Physiology. Cell Physiology*, *280*, C970–C979. https://doi.org/10.1152/ajpcell.2001.280.4.C970

Lambert, M., Boet, A., Rucker-Martin, C., Mendes-Ferreira, P., Capuano, V., Hatem, S., Adão, R., Brás-Silva, C., Hautefort, A., Michel, J. B., Dorfmuller, P., Fadel, E., Kotsimbos, T., Price, L., Jourdon, P., Montani, D., Humbert, M., Perros, F., & Antigny, F. (2018). Loss of KCNK3 is a hallmark of RV hypertrophy/dysfunction associated with pulmonary hypertension. *Cardiovascular Research*, *114*, 880–893. https://doi.org/10.1093/cvr/cvy016

Lambert, M., Capuano, V., Boet, A., Tesson, L., Bertero, T., Nakhleh, M. K., Remy, S., Anegon, I., Pechoux, C., Hautefort, A., Rucker-Martin, C., Manoury, B., Domergue, V., Mercier, O., Girerd, B., Montani, D., Perros, F., Humbert, M., & Antigny, F. (2019). Characterization of

Kcnk3-mutated rat, a novel model of pulmonary hypertension. *Circulation Research*, *125*, 678–695. https://doi.org/10.1161/CIRCRESAHA.119.314793

Lengyel, M., Czirjak, G., & Enyedi, P. (2016). Formation of functional heterodimers by TREK-1 and TREK-2 two-pore domain Potassium Channel subunits. *The Journal of Biological Chemistry*, *291*, 13649–13661. https://doi.org/10.1074/jbc.M116.719039

Lengyel, M., Czirjak, G., Jacobson, D. A., & Enyedi, P. (2020). TRESK and TREK-2 two-pore-domain potassium channel subunits form functional heterodimers in primary somatosensory neurons. *The Journal of Biological Chemistry*, *295*, 12408–12425. https://doi.org/10.1074/jbc.RA120.014125

Lengyel, M., Enyedi, P., & Czirjak, G. (2021). Negative influence by the force: Mechanically induced hyperpolarization via K2P background potassium channels. *International Journal of Molecular Sciences*, *22*, 9062. https://doi.org/10.3390/ijms22169062

Lengyel, M., Erdélyi, F., Pergel, E., Bálint-Polonka, Á., Dobolyi, A., Bozsaki, P., Dux, M., Király, K., Hegedűs, T., Czirják, G., Mátyus, P., & Enyedi, P. (2019). Chemically modified derivatives of the activator compound Cloxyquin exert inhibitory effect on TRESK (K2P18.1) background Potassium Channel. *Molecular Pharmacology*, *95*, 652–660. https://doi.org/10.1124/mol.118.115626

Lengyel, M., Hajdu, D., Dobolyi, A., Rosta, J., Czirják, G., Dux, M., & Enyedi, P. (2021). TRESK background potassium channel modifies the TRPV1-mediated nociceptor excitability in sensory neurons. *Cephalalgia*, *41*, 827–838. https://doi.org/10.1177/0333102421989261

Lilley, E., Stanford, S. C., Kendall, D. E., Alexander, S. P. H., Cirino, G., Docherty, J. R., George, C. H., Insel, P. A., Izzo, A. A., Ji, Y., Panettieri, R. A., Sobey, C. G., Stefanska, B., Stephens, G., Teixeira, M., & Ahluwalia, A. (2020). ARRIVE 2.0 and the British Journal of Pharmacology: Updated guidance for 2020. *British Journal of Pharmacology*, *177*(16), 3611–3616. https://doi.org/10.1111/BPH.15178

Lolicato, M., Arrigoni, C., Mori, T., Sekioka, Y., Bryant, C., Clark, K. A., & Minor, D. L. Jr. (2017). K2P2.1 (TREK-1)-activator complexes reveal a cryptic selectivity filter binding site. *Nature*, *547*, 364–368. https://doi.org/10.1038/nature22988

Ma, L., Roman-Campos, D., Austin, E. D., Eyries, M., Sampson, K. S., Soubrier, F., Germain, M., Trégouët, D. A., Borczuk, A., Rosenzweig, E. B., Girerd, B., Montani, D., Humbert, M., Loyd, J. E., Kass, R. S., & Chung, W. K. (2013). A novel channelopathy in pulmonary arterial hypertension. *The New England Journal of Medicine*, *369*, 351–361. https://doi.org/10.1056/NEJMoa1211097

Maingret, F., Patel, A. J., Lazdunski, M., & Honore, E. (2001). The endocannabinoid anandamide is a direct and selective blocker of the background K(+) channel TASK-1. *The EMBO Journal*, *20*, 47–54. https://doi.org/10.1093/emboj/20.1.47

Manoury, B., Lamalle, C., Oliveira, R., Reid, J., & Gurney, A. M. (2011). Contractile and electrophysiological properties of pulmonary artery smooth muscle are not altered in TASK-1 knockout mice. *The Journal of Physiology*, *589*, 3231–3246. https://doi.org/10.1113/jphysiol.2011.206748

Miller, P., Kemp, P. J., Lewis, A., Chapman, C. G., Meadows, H. J., & Peers, C. (2003). Acute hypoxia occludes hTREK-1 modulation: Re-evaluation of the potential role of tandem P domain K+ channels in central neuroprotection. *The Journal of Physiology*, *548*, 31–37.

Moha ou Maati, H., Veyssiere, J., Labbal, F., Coppola, T., Gandin, C., Widmann, C., Mazella, J., Heurteaux, C., & Borsotto, M. (2012). Spadin as a new antidepressant: Absence of TREK-1-related side effects. *Neuropharmacology*, *62*, 278–288. https://doi.org/10.1016/j.neuropharm.2011.07.019

Mondéjar-Parreño, G., Barreira, B., Callejo, M., Morales-Cano, D., Barrese, V., Esquivel-Ruiz, S., Olivencia, M. A., Macías, M., Moreno, L., Greenwood, I. A., Perez-Vizcaino, F., & Cogolludo, A. (2020). Uncovered contribution of Kv7 channels to pulmonary vascular tone in pulmonary arterial hypertension. *Hypertension*, *76*, 1134–1146. https://doi.org/10.1161/HYPERTENSIONAHA.120.15221

Montani, D., Seferian, A., Savale, L., Simonneau, G., & Humbert, M. (2013). Drug-induced pulmonary arterial hypertension: A recent outbreak. *European Respiratory Review*, *22*, 244–250. https://doi.org/10.1183/09059180.00003313

Murtaza, G., Mermer, P., Goldenberg, A., Pfeil, U., Paddenberg, R., Weissmann, N., Lochnit, G., & Kummer, W. (2017). TASK-1 potassium channel is not critically involved in mediating hypoxic pulmonary vasoconstriction of murine intra-pulmonary arteries. *PLoS ONE*, *12*, e0174071. https://doi.org/10.1371/journal.pone.0174071

Nagaraj, C., Li, Y., Tang, B., Bordag, N., Guntur, D., Enyedi, P., Olschewski, H., & Olschewski, A. (2022). Potassium channels in the transition from fetal to the neonatal pulmonary circulation. *International Journal of Molecular Sciences*, *23*, 4681. https://doi.org/10.3390/ijms23094681

Nagaraj, C., Tang, B., Balint, Z., Wygrecka, M., Hrzenjak, A., Kwapiszewska, G., Stacher, E., Lindenmann, J., Weir, E. K., Olschewski, H., & Olschewski, A. (2013). Src tyrosine kinase is crucial for potassium channel function in human pulmonary arteries. *The European Respiratory Journal*, *41*, 85–95. https://doi.org/10.1183/09031936.00211811

Nagaraj, C., Tang, B., Nagy, B. M., Papp, R., Jain, P. P., Marsh, L. M., Meredith, A. L., Ghanim, B., Klepetko, W., Kwapiszewska, G., Weir, E. K., Olschewski, H., & Olschewski, A. (2016). Docosahexaenoic acid causes rapid pulmonary arterial relaxation via KCa channel-mediated hyperpolarisation in pulmonary hypertension. *The European Respiratory Journal*, *48*, 1127–1136. https://doi.org/10.1183/13993003.01814-2015

Nagy, B. M., Nagaraj, C., Meinitzer, A., Sharma, N., Papp, R., Foris, V., Ghanim, B., Kwapiszewska, G., Kovacs, G., Klepetko, W., Pieber, T. R., Mangge, H., Olschewski, H., & Olschewski, A. (2017). Importance of kynurenine in pulmonary hypertension. *American Journal of Physiology. Lung Cellular and Molecular Physiology*, *313*, L741–L751. https://doi.org/10.1152/ajplung.00517.2016

Olschewski, A., Li, Y., Tang, B., Hanze, J., Eul, B., Bohle, R. M., Wilhelm, J., Morty, R. E., Brau, M. E., Weir, E. K., Kwapiszewska, G., Klepetko, W., Seeger, W., & Olschewski, H. (2006). Impact of TASK-1 in human pulmonary artery smooth muscle cells. *Circulation Research*, *98*, 1072–1080. https://doi.org/10.1161/01.RES.0000219677.12988.e9

Olschewski, A., Papp, R., Nagaraj, C., & Olschewski, H. (2014). Ion channels and transporters as therapeutic targets in the pulmonary circulation. *Pharmacology & Therapeutics*, *144*, 349–368. https://doi.org/10.1016/j.pharmthera.2014.08.001

Pandit, L. M., Lloyd, E. E., Reynolds, J. O., Lawrence, W. S., Reynolds, C., Wehrens, X. H., & Bryan, R. M. (2014). TWIK-2 channel deficiency leads to pulmonary hypertension through a rho-kinase-mediated process. *Hypertension*, *64*, 1260–1265. https://doi.org/10.1161/HYPERTENSIONAHA.114.03406

Papp, R., Nagaraj, C., Zabini, D., Nagy, B. M., Lengyel, M., Skofic Maurer, D., Sharma, N., Egemnazarov, B., Kovacs, G., Kwapiszewska, G., Marsh, L. M., Hrzenjak, A., Höfler, G., Didiasova, M., Wygrecka, M., Sievers, L. K., Szucs, P., Enyedi, P., Ghanim, B., … Olschewski, A. (2019). Targeting TMEM16A to reverse vasoconstriction and remodelling in idiopathic pulmonary arterial hypertension. *The European Respiratory Journal*, *53*, 1800965. https://doi.org/10.1183/13993003.00965-2018

Patel, A. J., Honoré, E., Maingret, F., Lesage, F., Fink, M., Duprat, F., & Lazdunski, M. (1998). A mammalian two pore domain mechano-gated S-like K+ channel. *The EMBO Journal*, *17*, 4283–4290. https://doi.org/10.1093/emboj/17.15.4283

Percie du Sert, N., Hurst, V., Ahluwalia, A., Alam, S., Avey, M. T., Baker, M., Browne, W. J., Clark, A., Cuthill, I. C., Dirnagl, U., Emerson, M.,

Garner, P., Holgate, S. T., Howells, D. W., Karp, N. A., Lazic, S. E., Lidster, K., MacCallum, C. J., Macleod, M., … Würbel, H. (2020). The ARRIVE guidelines 2.0: updated guidelines for reporting animal research. *PLoS Biology*, *18*(7), e3000410. https://doi.org/10.1371/journal.pbio.3000410

Platoshyn, O., Golovina, V. A., Bailey, C. L., Limsuwan, A., Krick, S., Juhaszova, M., Seiden, J. E., Rubin, L. J., & Yuan, J. X. J. (2000). Sustained membrane depolarization and pulmonary artery smooth muscle cell proliferation. *American Journal of Physiology. Cell Physiology*, *279*, C1540–C1549. https://doi.org/10.1152/ajpcell.2000.279.5.C1540

Platoshyn, O., Remillard, C. V., Fantozzi, I., Mandegar, M., Sison, T. T., Zhang, S., Burg, E., & Yuan, J. X. J. (2004). Diversity of voltage-dependent K+ channels in human pulmonary artery smooth muscle cells. *American Journal of Physiology. Lung Cellular and Molecular Physiology*, *287*, L226–L238. https://doi.org/10.1152/ajplung.00438.2003

Skofic Maurer, D., Zabini, D., Nagaraj, C., Sharma, N., Lengyel, M., Nagy, B. M., Frank, S., Klepetko, W., Gschwandtner, E., Enyedi, P., Kwapiszewska, G., Olschewski, H., & Olschewski, A. (2020). Endothelial dysfunction following enhanced TMEM16A activity in human pulmonary arteries. *Cells*, *9*, 1984. https://doi.org/10.3390/cells9091984

Sun, H., Xia, Y., Paudel, O., Yang, X. R., & Sham, J. S. (2012). Chronic hypoxia-induced upregulation of Ca2+−activated cl- channel in pulmonary arterial myocytes: A mechanism contributing to enhanced vasoreactivity. *The Journal of Physiology*, *590*, 3507–3521. https://doi.org/10.1113/jphysiol.2012.232520

Tang, B., Li, Y., Nagaraj, C., Morty, R. E., Gabor, S., Stacher, E., Voswinckel, R., Weissmann, N., Leithner, K., Olschewski, H., & Olschewski, A. (2009). Endothelin-1 inhibits background two-pore domain channel TASK-1 in primary human pulmonary artery smooth muscle cells. *American Journal of Respiratory Cell and Molecular Biology*, *41*, 476–483. https://doi.org/10.1165/rcmb.2008-0412OC

Yuan, J. X., Aldinger, A. M., Juhaszova, M., Wang, J., Conte, J. V. Jr., Gaine, S. P., Orens, J. B., & Rubin, L. J. (1998). Dysfunctional voltage-gated K+ channels in pulmonary artery smooth muscle cells of patients with primary pulmonary hypertension. *Circulation*, *98*, 1400–1406. https://doi.org/10.1161/01.CIR.98.14.1400

Yuan, X. J., Wang, J., Juhaszova, M., Gaine, S. P., & Rubin, L. J. (1998). Attenuated K+ channel gene transcription in primary pulmonary hypertension. *Lancet*, *351*, 726–727. https://doi.org/10.1016/S0140-6736(05)78495-6

SUPPORTING INFORMATION

Additional supporting information can be found online in the Supporting Information section at the end of this article.

How to cite this article: Csáki, R., Nagaraj, C., Almássy, J., Khozeimeh, M. A., Jeremic, D., Olschewski, H., Dobolyi, A., Hoetzenecker, K., Olschewski, A., Enyedi, P., & Lengyel, M. (2024). The TREK-1 potassium channel is a potential pharmacological target for vasorelaxation in pulmonary hypertension. *British Journal of Pharmacology*, *181*(19), 3576–3593. https://doi.org/10.1111/bph.16426